B.A.R.C.-1469

सत्यमेव जयते

A REPORT ON
DIGITAL IMAGE PROCESSING AND ANALYSIS

by

B. Singh, J. Alex and G. Haridasan
Ultrasonic Instrumentation Section
Electronics Division

1989

B.A.R.C. - 1469

B.A.R.C. - 1469

A REPORT ON DIGITAL IMAGE PROCESSING & ANALYSES

by

B. Singh, J. Alex and G. Haridasan
Ultrasonic Instrumentation Section
Electronics Division

Preface

This report presents our developments in software, connected with digital image processing & analysis.

In image processing, we resort to either alteration of grey level values so as to enhance features in the image or we resort to transform domain operations for restoration or filtering. Typical transform domain operations like Karhunen-Loeve transforms are statistical in nature and are used for a good registration of images or template - matching. Image - Analysis procedures segment grey - level images into images contained within selectable windows, for the purpose of estimating geometrical features in the image, like area, perimeter, projections etc.

In short in image processing both the input and output are images, whereas in image analyses, the input is an image whereas the output is a set of numbers and graphs.

ACKNOWLEDGMENTS

Chapter	Contents	Page

DIGITAL IMAGE PROCESSING & ANALYSES

I. INTRODUCTION

GENERALIZED IMAGING SYSTEMS :- Imaging systems can produce
only an imperfect replica of an object. Even when the imaging
system is perfect and the imaging conditions are ideal, the
phenomenon of diffraction limits the closeness of an object to
its image. In reality, the defects in the imaging system
(aberration, coma, etc.) and pre imaging conditions often
severely limit the quality of images obtained . To improve the
quality, there are two approaches: image-enhancement and image
restoration. An attempt is made to make the images "look" better
than the original in the first approach. In order to achieve
this, techniques like contrast stretching & histogram
equalization (described later) are adopted. In the second
approach, an attempt is made to "invert" the degradation
processes so that a good estimate of the object is obtained. The
degradative processes could be modeled in the following manner.
Intensity at a point in the image is contributed by all points in
the object to a greater or lesser degree. This phenomenon is the
well known Diffraction - effect. When the imaging aperture is
ci_cular, a point source gives rise to a blurred image. The
blurring effect can be removed by deconvolution procedures
(discussed later) and a better quality image could be obtained.

IMAGE ENHANCEMENT AND IMAGE RESTORATION:

Enhancement is the attempt to improve the appearance of an image for human viewing or subsequent machine processing. In this case there does not exist an 'ideal' image, as in the case of image restoration. Examples of enhancement techniques would be the pseudocolouring of images that are monochrome and the emphasizing of contrasts in the image. Mathematically, two dimensional grey tone images can be described by a brightness or intensity function I, whose value varies with the location (x,y) in the image plane.

I = f(x,y)

'I' may take a continuous range of values as in most natural images acquired by analog means or a limited number of discrete values. The various values taken by 'I' in a monochrome (grey-tone) image are known as 'grey-levels' and are graded in increasing intensity from black to white.

Image enhancement involves the transformation of intensity function of a given image with a view to increasing the quality of the image. Practical image forming systems have limited resolution and so it is permissible (without loosing too much information) to scan a picture line by line, as in television scanning to convert the image into a time-series signal. The picture or image can also be described as a two dimensional matrix of discrete individual pixels, whose values vary from one pixel to another. Scanning and two dimensional sampling are thus

two important preludes to image -processing -operations.

Digital enhancement comprises of three main categories of processing operations:

i) Geometric or address dependent operations.

ii) Point or pixel operations and

iii) Neighbourhood operations.

Examples of geometric operations are image translation, rotation and magnification. Such processing may serve to correct for distortion. Point operations are carried out in the same way for each picture element in the image, independent of its position or the value of its neighbouring elements .e.g., log compression, histogram modification, arithmetic combinations, Boolean combinations, etc,. Neighbourhood operations modify the value of the pixel in a way that depends on the intensity values of the neighbouring pixels.

Other sources of degradation are relative motion between the object and the imaging system (medical images - computed tomographic images), turbulence in the medium between the object and the imaging system (astronomical images), object plane not normal to the axis of the imaging system, etc. All these will effect the PSF's and will degrade the images generated.

Restoration is that process in which the computer is used to invert some degradation phenomena that the image has suffered in the process of formation. For example, blurring or geometric

distortion is to be studied & linked to various causes, mathematical model is formulated and then a process to invert this degradation is worked out. Thus using restoration techniques it is possible to restore an image that has suffered the ill effects, of say, transmission through atmospheric turbulence or a fault in the focusing of the imaging system, as closely as possible to an 'ideal' image.

Let us denote object -plane and image -plane as $f(x,y)$ and $g(x',y')$ respectively and the point spread function by $h(x,y,x',y')$ -as the contribution of a " point source at coordinates x,y in the object space" to the pixel at x',y' in the image. Thus the image $g(x',y')$ can be written as

$$g(x',y') = \int \int f(x,y).h(x',y',x,y) \, dx \, dy + n(x',y') \qquad (1)$$

where $n(x',y')$ denotes "noise".

A significant point to remember is that the PSF is an indicator of the quality of images and when PSF is narrower, the degradation is minimal.

Turbulence in the medium is difficult to model correctly. For example the atmospheric turbulence will cause changes in the refractive index of the medium. Astronomical images will thus be subjected to degradative processes, which are uncontrollable. Using the arguments of Central Limit theorem, the PSF may be

shown to obey Gaussian distribution. Thus,

$$h(x,x',y,y') = 1/\sqrt{2}\Pi\sigma \times \exp[-\{(x-x')^2+(y-y')^2\}/2\sigma^2] \qquad (2)$$

when the axis of the imaging system is at an angle to the normal, the nature of PSF will be point-source dependent. Such PSF's are called shift variant PSF's. Image restoration techniques are broadly classified into - techniques for shift invariant and that for shift variant PSF's.

Shift Invariant PSF & Restoration:

When the PSF is shift invariant, the integral in equation (1) becomes a convolution. Thus

$$g(x,y) = f(x,y) * h(x,y) \qquad (3)$$

where * denotes the convolution operation.

Taking Fourier transform, we have

$$G(w_x,w_y) = F(w_x,w_y) . H(w_x,w_y) \qquad (4)$$

where w_x , w_y refers to spatial frequencies.

Thus,

$$F(w_x,w_y) = G(w_x,w_y) / H(w_x,w_y) \qquad (4)$$

As, the RHS is known, $F(w_x,w_y)$ could be determined. Taking the inverse transform we have $f(x,y)$. This operation is called ideal inverse filtering. However, when the noise term is taken into account, we obtain only an estimate of $f(x,y)$. When the effect of noise predominates in a given image, inverse filtering techniques become unstable, particularly when $H(w_x,w_y)$ becomes smaller. It is here that Wiener estimation theory becomes useful. Wiener filtering estimates the filter coefficients statistically using

5

power spectral methods. Such of those minimum error coefficients are employed to obtain the so called "Wiener filters".

It can be easily seen that statistical variability is computed from past values of the time series, to predict the values of the coefficients. The approach adopted for realizing Wiener filtering assumes that the power spectral densities are very well known and the time series is in a wide sense stationary. Both are open to question and so a number of other interactive tunable filters are used.

Shift Variant PSF & Restoration:

When the PSF is shift variant, equation (1) can not be simplified: and the restoration task becomes much more difficult. Many interactive techniques are being tried out for this purpose and we shall not elaborate this topic any further.

II GREY LEVEL PROCESSING (POINT OPERATIONS)

An image is a two dimensional representation of information, and it is represented as a function of the space coordinates (x,y). Such a continuous function of x and y is sampled at regular intervals of x and y and the sample values (corresponding to the intensity at that point) are approximated to the nearest integers. The integers are given binary representation and stored in the form of a matrix of finite dimensions, i.e., intensity (grey scale) at the point (i,j) is denoted by im(i,j) where i,j are integers and im(i,j) is an integer array. Some basic properties of images are:

(I)   im(i,j) > = 0 for all i,j

(II)   im(i,j) < = M for all i,j

(III) im(i,j) = 0 for i > N or j > N where N x N is the total number of points to which the image is digitized.

Image processing or picture processing can be defined rather widely. It encompasses all the following :

a) Picture digitisation and coding : conversion of pictures from continuous to discrete form; and compaction of the resulting image for efficient storage and transmission.

b) Picture restoration and enhancement : Improvement of degraded pictures and increasing the quality of images (discussed earlier in chapter I).

c) Picture segmentation and description : **Transforming** an image to yield a decision or a set of parameters that characterizes it completely.

The aim of image processing is to enhance the signal to noise ratio and to extract hidden information. The topic 'image processing' covers essentials of digital picture processing, pattern recognition, feature extraction, image enhancement and standardization procedures for the purpose of improving the quality of images.

Generally image or picture processing are discussed under two categories: i) pre-processing and ii) post processing. Pre-processing is specific to the modality of generating pictures. For example in ultrasonic imaging, the video signals are routed through a PROM-lookup-table to compensate for the logarithmic attenuation of ultrasound.

Post processing refers to the processes carried out to the data or information in the main memory. Processing of such data (spatial or array processing) is considered either for statistically processing the information or analyzing the image by converting the grey level images into binary images. (Discussed later). Technical requirement of **REAL TIME** processes are stringent as processing is required to be completed within 20 milliseconds.

DESCRIPTION OF AN IMAGE FROM STATISTICAL ANGLE:

An image will consists of N x M pixels arranged in an array. Each pixel shall contain an intensity level. A histogram of an image is a plot of the number of pixels in each grey level, which denotes the probability of occurrence in a gray-level. It is called the statistical descriptor of an image. See Fig. 2.1 for the probability density distributions in a typical grey level image. Fig. 2.2 gives the cumulative density function (CDF) for the same image.

To evaluate a histogram, we treat grey levels as discrete and scale down the number of pixels so that the histogram represents the probability density function of the grey level distribution. Each point on the curve will represent the probability that a pixel has that particular grey level value.

The area under the histogram or the probability density function (PDF) is invariant. In the case of histogram it is always equal to the total number of pixels in the image. The PDF is scaled down in such a way that the area is always equal to unity (which is consistent with the statistical definition of a PDF).

HISTOGRAM MODIFICATION

The basis of histogram modification is one of redistribution of pixel values such that the area under PDF curve remains the same. The average brightness of the original image is given by ,
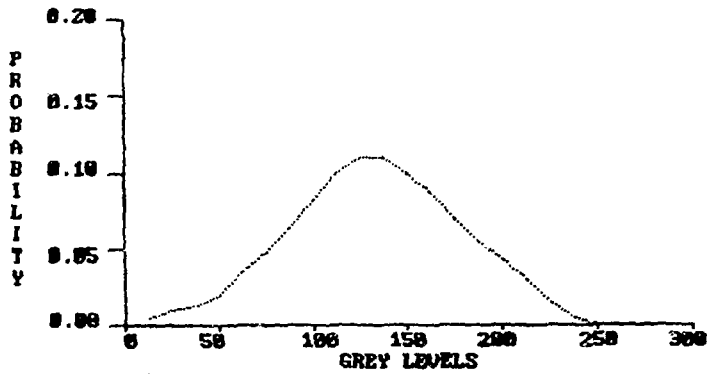
9

Fig. 2.1 Probability density function for grey level in a
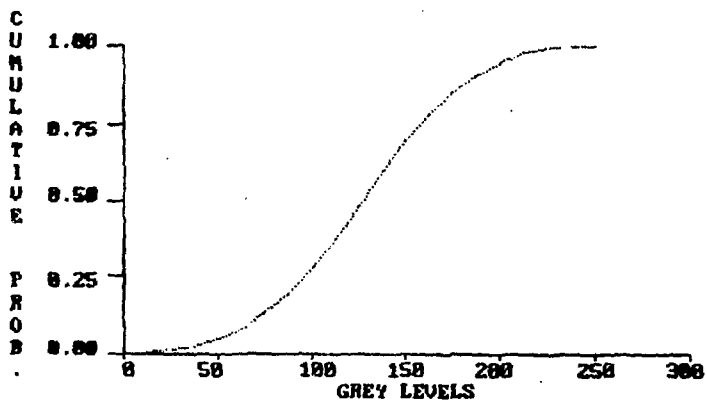typical picture.

Fig. 2.2 Cumulative density function (CDF) for the probability
density shown in fig 2.1.

10

$$X' = \int_0^1 x \, p(x) \, dx \, ,$$

while the contrast σ by

$$\sigma^2 = \int_0^1 (x-x')^2 \, p(x) \, dx$$

Hence by changing the histogram $P(x)$, we can alter the brightness, contrast, etc.

Histogram Modification

Let $P(x)$ be the PDF of the original image and $P(x_1)$ the probability that a pixel in the original image contains the grey level x_1. Let $P(y)$ be the desired PDF or the histogram ; where 'y' represents the grey levels of the enhanced image. We have the equality,

$$\int_0^x Px(s) \, ds = \int_0^y Py(s) \, ds = 1 \quad \text{for the CDFs. (See Fig. 2.3)}$$

It is evident from the above figure, that Y can be obtained as a function of X. The integral $\int_0^y Py(s) \, ds$ can also be looked upon as a transformation on Y. Hence we may write,

$$G(Y) = \int_0^y Py(s) \, ds$$

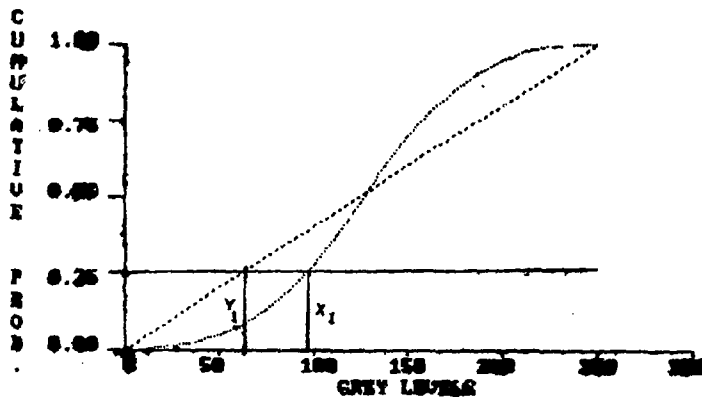To find Y, we need only to find the inverse transformation of G.

Fig. 2.3 Cumulative density functions for two images of
different grey level distributions. To generate
the LUT for grey level transformation, a table
is prepared for X_1 against Y_1 for the
same CDF values.

$$Y = G^{-1}(G(Y))$$

$$= G^{-1}\left[\int_0^y Py(s)\ ds \right]$$

$$= G^{-1}\left[\int_0^x Py(s)\ ds \right]$$

This equation is the required transfer function between X and Y. The same algorithm is illustrated geometrically (See Fig. 2.3). It also gives a better insight into the problem. Cumulative density function (CDF) are drawn on the same graph as can be drawn choosing the same coordinates for both X and Y as shown in fig. 2.3. We have for each X(say $x = x_1$) the value for $\int Px(s)\ ds$ and also we find the value of $\int Py(s)\ ds$ which equals the value of $CDF(x_1)$. The value of Y for which CDF of Y equals CDF of X is the required transformation between X and Y.

HISTOGRAM EQUALIZATION

It is a special case of histogram modification for image enhancement. Here the Py(Y) is a uniform PDF. It means we desire equal probability of occurrence for all the grey levels. Equalization of the histogram improves the quality of an image by redistributing its pixels uniformly over the entire grey level range. That is , if {Ai}(i=1 to K1) represents the grey levels of the input histogram and {Bj}(j=1 to K2) then,

$$\sum_{i=1}^{k1} Ai = \sum_{j=1}^{k2} Bj \quad \text{and } k1/k2 = N(\text{integer}), \; Bj = \sum_{i1}^{i2} Ai$$

The result is an array transforming every subset of {Ai} to an unique Bi. As equiprobable distribution of pixels yields maximum information , the resultant image can reveal hidden features.

Fig. 2.4(a) shows the photograph of a girl. It can be seen that details of facial features are absent. We shall demonstrate that by adopting histogram equalization procedure, such details can be restored, to large extent. The input image has the grey level distribution between 100 and 255. During the processing schedule histogram is equalized such that the entire gray level range is occupied. The processed image is shown in Fig. 2.4(b) that looks much better, even when it is displayed in 8 gray shades and printed on a dot matrix printer. A comparison of Fig. 2.4(a) and 2.4(b) shows that the hidden details are extracted and the processed picture contains more visual information to any observer.

As we indicated earlier, the grey level distribution (GLD) is the statistical descriptor of an image. The manner in which it can be modified can be specified by a transformation function. The transformation can be specified by any of the following functions - linear, exponential or non - linear, as illustrated in Fig. 2.5. When a raw image is subjected to any one of the above transformation, the image data or the matrix is altered,

14

2.4 Histogram of results along with the
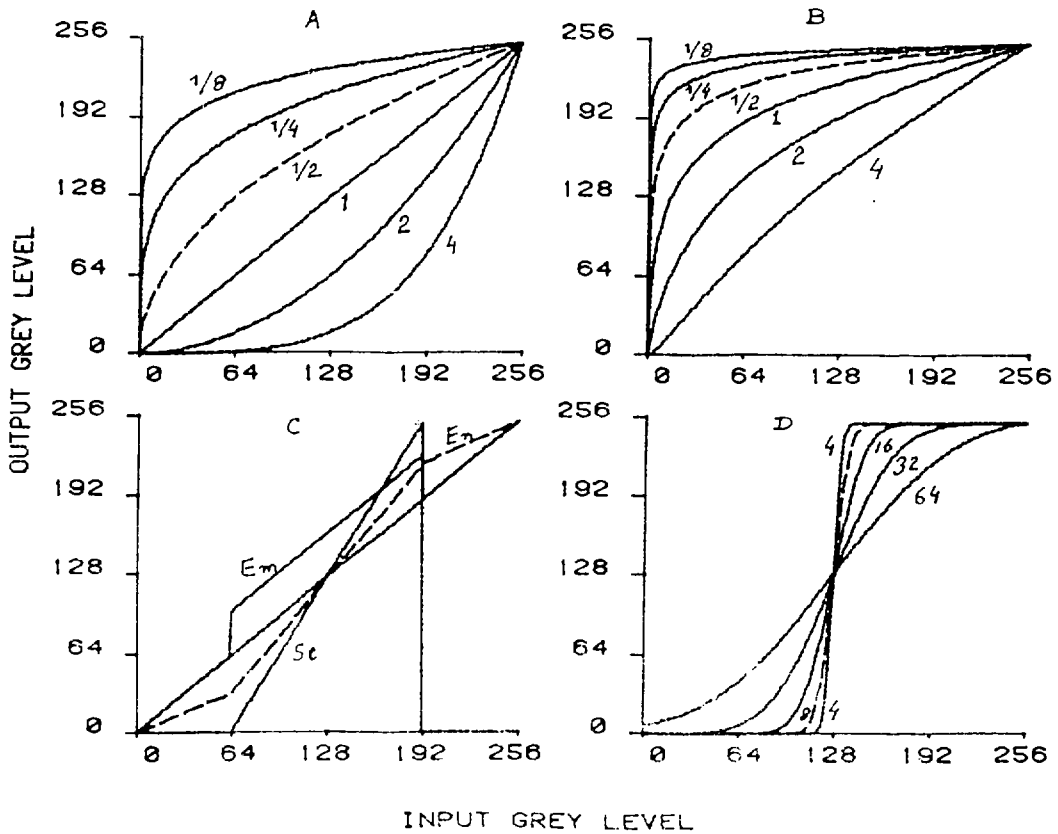grey level distribution of the digitised image
are plotted.
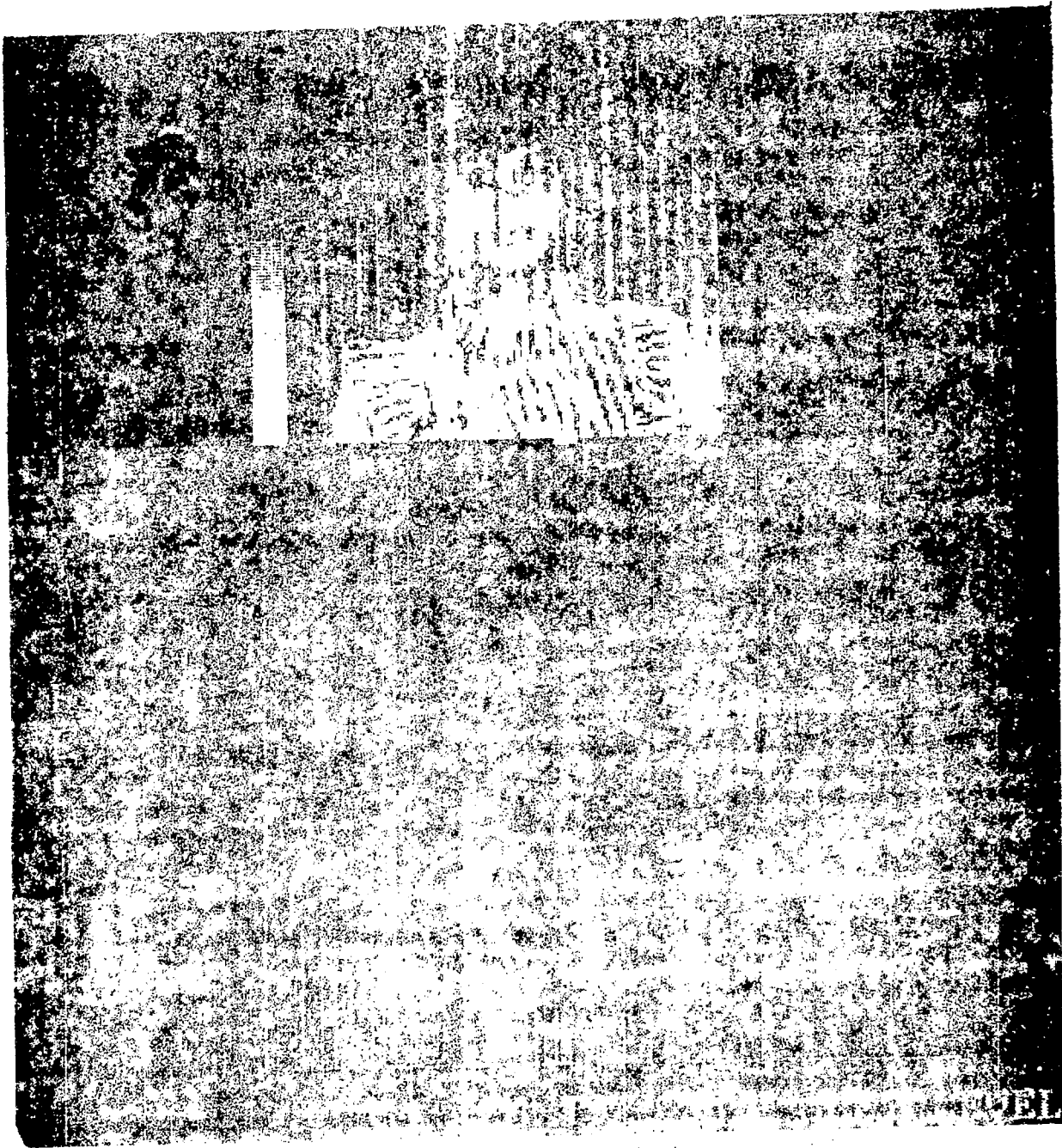
Fig 2.5 : Input output relation between pixel intensities,
called transfer functions, are depicted for different
schemes of transformation.
A : Output based on the power (X**N) of input grey level
for different values (4,2,1,1/2,1/4,1/8) of N.
B : Output based on the power [log(1+X)]**N of input grey
level for different values (4,2,1,1/2,1/4,1/8) of N.
C : Modification restricted to the user defined grey level
window, Em - emphasis, En - enhancement, St -
stretching.
D : Sigmoid shaped of transfer function controlled by a
Gaussian function, mean=128, and different values of
S.D.: S1=64, S2=32, S3=16, S4=8, S5=4.

17

or redistributed in its value. That is to say, the pixel intensities of the processed image get altered as specified by the input-output transformation relations.

Fig. 2.6 shows a sector scan image of kidney, in black and white. The grey levels in the raw image span from 0-200. Those pixels whose grey levels lies within the window 100 to 180 are stretched to occupy the levels 0-255 in the processed Image. Notice that the boundary of the internal organ is highly pronounced in the processed image.

In Fig. 2.7 the left bottom quadrant of the raw image (shown in Fig. 2.6) is depicted to a magnified scale. The original image with window corresponding to that quadrant is also shown on RHS. The grey levels in the regions of interest(ROI),from 100-180 levels are stretched to occupy 0-255. Such operations are employed to scrutinize magnified areas.
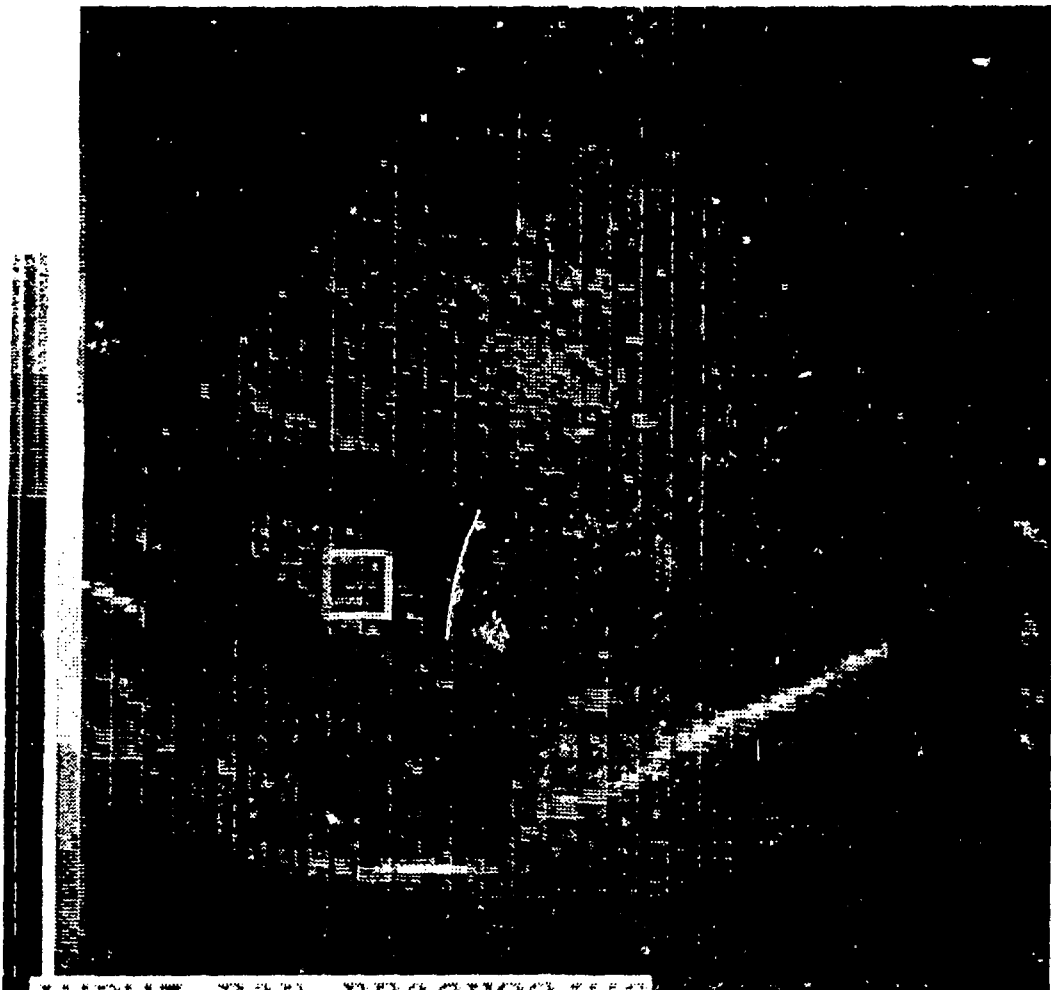
Fig. 2.6-a: Raw image (ultrasonic sector scan of kidney recorded in 35mm film & digitized using densitometer of 8 bit resolution, or 256 levels). Print out on dot matrix printer, 8 grey shades. Grey-level histogram of raw image is shown in the lower part.

19

HISTOGRAM ALTERATION STRETCHING

Fig. 2.6-b: Processed image where grey level stretching is
effected. Levels 100-180 in Fig-a have been stretched
to occupy 0-255 levels. Print out on dot matrix
printer, 8 grey shades, generated. Grey-level
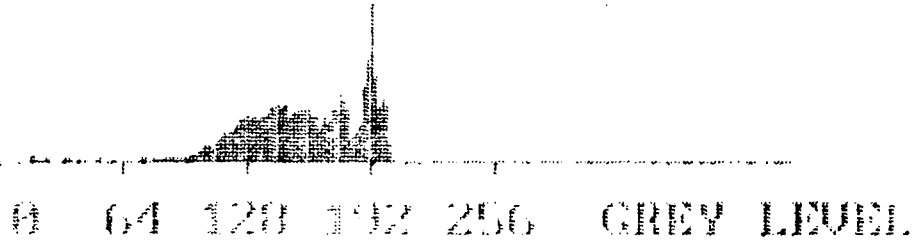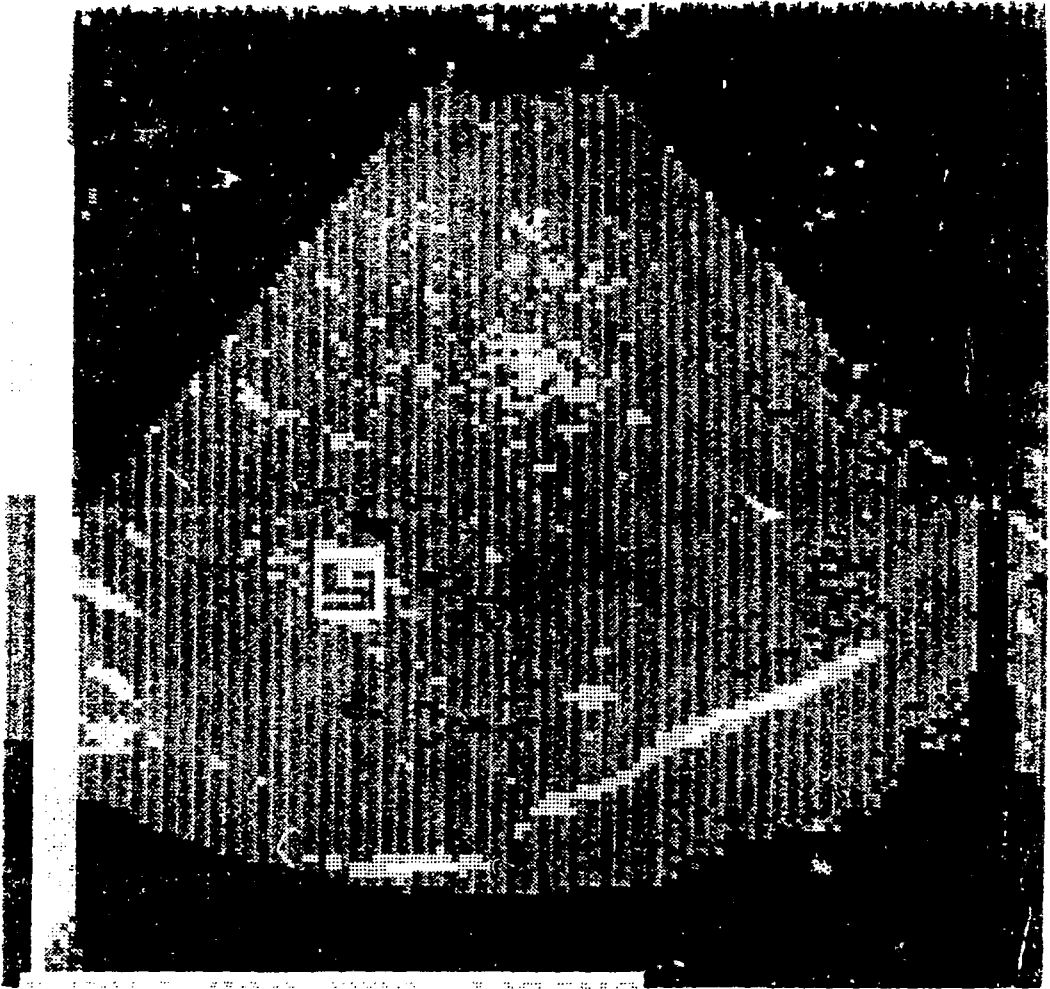histogram of processed image is shown in lower part.

20

Fig. 2.6-c: Raw image (ultrasonic sector scan of kidney recorded
in 35mm film & digitized using densitometer of 8 bit
resolution, or 256 levels). Print out on dot matrix
printer, 4 grey shades, generated. Grey-level
histogram of raw image is shown in lower part.

Fig. 2.6-d: Processed image where grey level stretching is
          effected. Levels 100-180 in Fig-a have been stretched
          to occupy 0-255 levels. Print out on dot matrix
          printer, 4 grey shades, generated. Grey-level
          histogram of processed image is shown in lower part.

22

Fig 2.7 : Region of interest processing is depicted in this
          figure. Input image is the same as in the previous
          figure.
   2.7-a: One quadrant of original image is shown magnified.
   2.7-b: Raw image(Ultrasonic sector scan of Kidney recorded
          in 35mm film & digitized using densitometer of 8 bit
          resolution or 256 levels. Bottom left quadrant is
          shown negated.)
   2.7-c: Processed (quadrant) image. Grey level stretching
          operation (100 - 180 levels of Fig -a have been
          stretched to 0 - 255).
   2.7-d: Grey level histogram of Fig -c.

III TRANSFORM DOMAIN OPERATIONS (GLOBAL OPERATIONS).

Image matrices are transformed into various domains for easy handling of images such as coding, compaction & transmission. Such transform domain filtering operations are mathematically well defined.

Frequency Domain Filtering

From the general theory of signal dynamics, it is known that convolution achieves filtering. Also, convolution operation in the time domain is equivalent to multiplication in the frequency domain and vice versa.

The impulse response function of a system yields information on the time domain response for an ideal impulse-input. By inverse transform relationship, we say that the frequency domain characteristics of a system could be analyzed by using white noise as the input source. To put in mathematically, one dimensional relation can be written as -

$G(w) = H(w).F(w)$

where $G(w)$ is the frequency characteristics of the system.

$H(w)$ is the fourier transform of white noise which is unity and $F(w)$ is the frequency domain characteristics of the input signal. As $H(w) = 1$ and $G(w) = F(w)$
and hence we call such a filter as "matched filter". All these arguments are valid only for ideal (no noise) situations.

Filtering operation in general involves permitting certain

frequency components and suppressing the unwanted. The experimenter's interest in specific problems will dictate such considerations. Preferential selection of frequency components would highlight the nature of images when other components are totally absent. Thus unlike the grey level operations, we can smoothen, deblur or differentiate the picture to alter its frequency contents or to enhance or highlight hidden details. It should be realized that in all practical systems, presence of noise is inevitable and the source of noise could be identified and noise minimized right at the source. Noise could be picture independent, picture dependent, uncorrelated point to point, and also in some cases coherent. We assume the systems to be linear, shift - invariant and use unweighted averaging for all our processing operations. We consider "additive noise", which could be reduced by signal averaging. "Convolved noises" require deconvolution procedures and are not described in this report.

During filtering operation specific frequency-bands could be chosen or suppressed, thus making the operation flexible. Such operations are globally sensitive as spectral estimation is carried out for the image, as a whole. In filtering operations, the chosen   "transfer function" will determine the characteristics of the processed image.

Fig. 3.1 depicts a model of a square containing a circle within. Fourier transform of the model is depicted in 3.1(c).

Fig 2 7   Region of interest processing is depicted in this figure   Input image is the same as in the previous
           figure
    2 7 a One quadrant of original image is shown magnified
    2 7 b Raw image (Ultrasonic sector scan of kidney recorded in 35mm film & digitized using densitometer of
           8 bit resolution or 256 levels Bottom left quadrant is shown negated)
    2 7 c Processed (quadrant) image   Grey level stretching operation (100 - 180 levels of Fig a have been
           stretched to O   255)
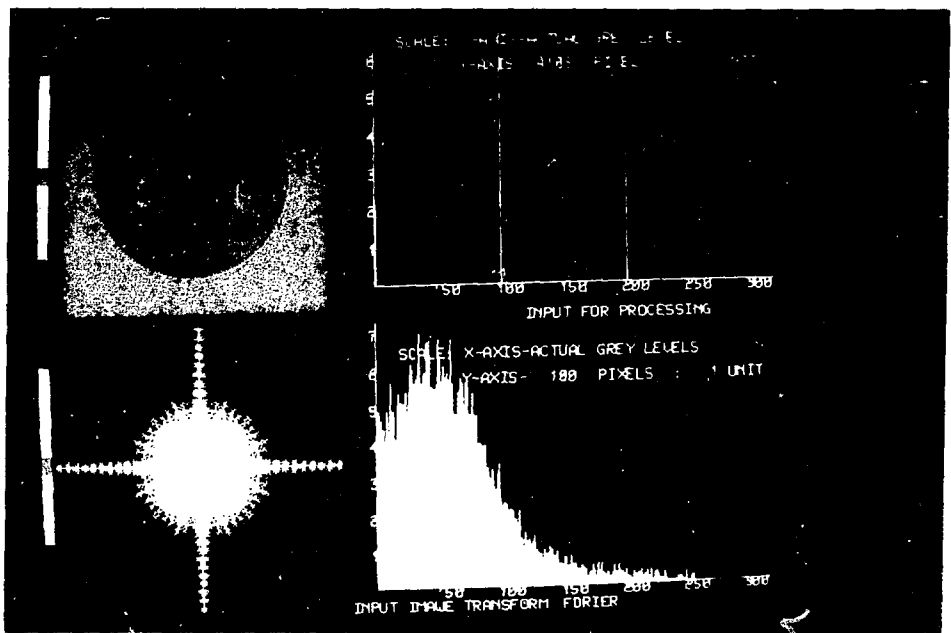   2 7 d Grey level histogram of Fig c

Fig 3 1 a Modelled geometric object a square containing a circle
    3 1 b Greylevel histogram of Fig a
    3 1 c Fourier transform of the image a
    3 1 d Grey level histogram of Fig j

Corresponding grey level distributions are shown in 3.1(b) & 3.1(d) respectively. Note the symmetrical repeat patterns of spatial frequency distribution in 3.1(b). Maximum information is contained in a very small region around the center (zero frequency). Two specific pseudo colour are assigned for the geometrical figures. The Grey Level distribution shows accordingly only two distinct distribution.

We shall now consider salient features of specific filters used in image processing application.

Ideal filter: This filter is of academic interest alone. Box - like transfer function is difficult to implement, although selectable in softwares. But as the transient effects also called Gibb's phenomenon, are difficult to eliminate, they are seldom employed, exclusively. However, Hanning and Hamming operations which will reduce such effects, are employed in practice. Fig. 3.2 depicts the frequency characteristics of such filter.

Trapezoidal filter: This filter is a modified version of ideal filter, where the transition band is increased which consequently reduces the Gibb's phenomenon.

A geometrical object is modeled (in ND 560 system) as shown in Fig. 3.3(a). A trapezoidal filter operates on the raw image, to eliminate high frequency noise. It can be seen that background noise has been suppressed, to a great extent but the edges in
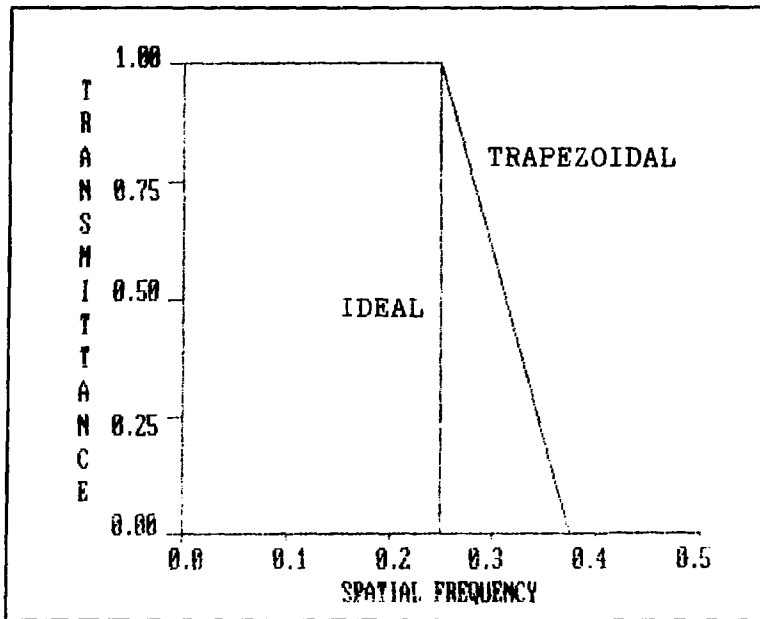
27

Fig. 3.2   : Frequency characteristics - Ideal and trapezoidal filters. (one dimensional representation)
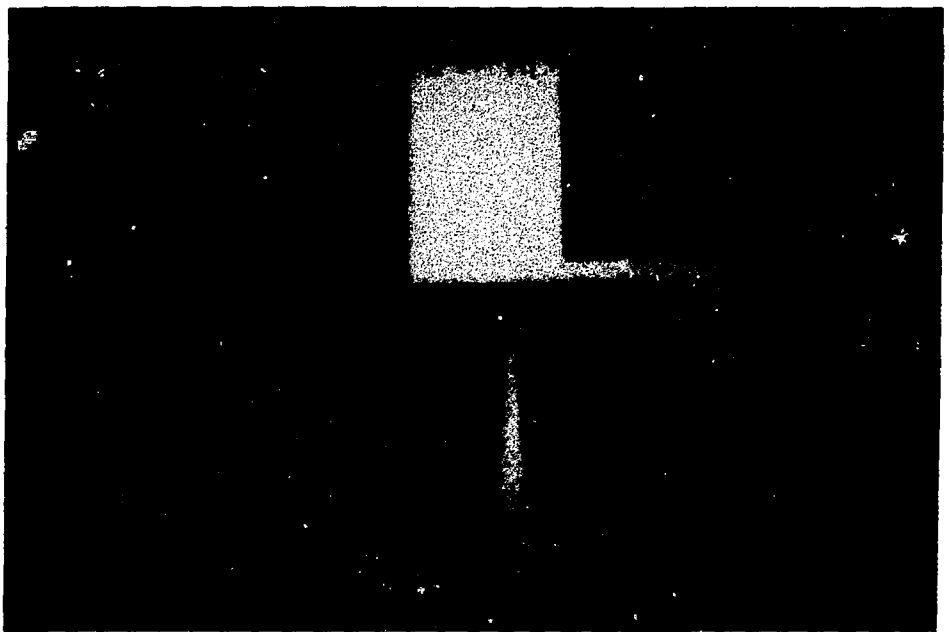

Fig. 3.3-a : Modelled image of noisy geometrical objects.
    3.3-b : Greylevel histogram of Fig - a.
    3.3-c : Image obtained by Trapezoidal L.P. filtering. (transition band 25/120-50/120)
    3.3-d : Grey level histogram of Fig-c.

the geometrical figure appear corrugated in the processed image. Fig 3.3(b) and Fig. 3.3(d) show respective grey level distribution. The importance of low pass trapezoidal filtering is that it eliminates "noise", by cutting down higher frequency components but (because of averaging effect) the edges are no longer preserved with sharp features, as depicted in Fig. 3.3(c).

Butterworth Filter: For a monotonous and maximally flat response at zero frequency, the Butterworth filter is chosen. The transfer function variations near the cut off are not sharp. In the stop band the transfer function rolls off at -6dB per octave per order n of the filter, thus monotonously decreasing to zero at higher frequencies. See Fig. 3.4 for the frequency characteristics of a butterworth filter, in 1 - dimension.

A raw image (Kidney sector scan) & the Fourier domain representation of the image convolved with Butterworth low pass filter are depicted in Fig. 3.5(a) & (b). The Fourier transform of the image is multiplied with the transfer function of Butterworth low pass filter and the product is depicted in Fig. 3.5(b) in the frequency domain. The respective GL distributions are shown in Fig. 3.5(c) and Fig. 3.5(d). The Fourier domain representation shows that the information is located around the zero or dc value. Fig. 3.6(b) depicts, in a similar manner, the change that result in the image when subjected to trapezoidal filtering. The processed image depicts additional details not
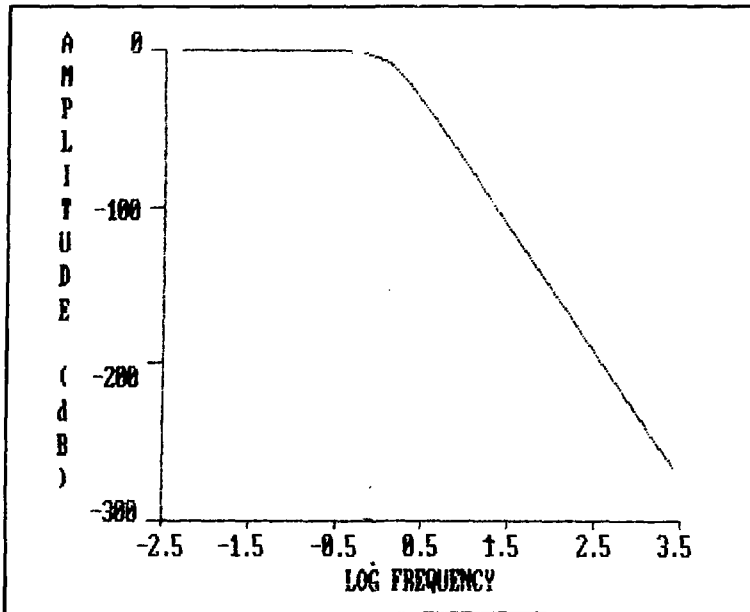
29

Fig. 3.4 : Butterworth filter characterisitics for 2nd order
filter. The stop band roll off is -12dB/octave. The cutoff
is at frequency 1.0 (log Fc = 0.0)

Fig. 3.5-a : Raw image (Ultrasonic sector scan of kidney recorded in 35 mm film & digitized using densitometer
of 8 bit resolution or 256 levels).
3.5-b : Product of Fourier Transform of Fig - a with T.F. of Butterworth low pass filter.
3.5-c : Grey level histogram of Fig -a.
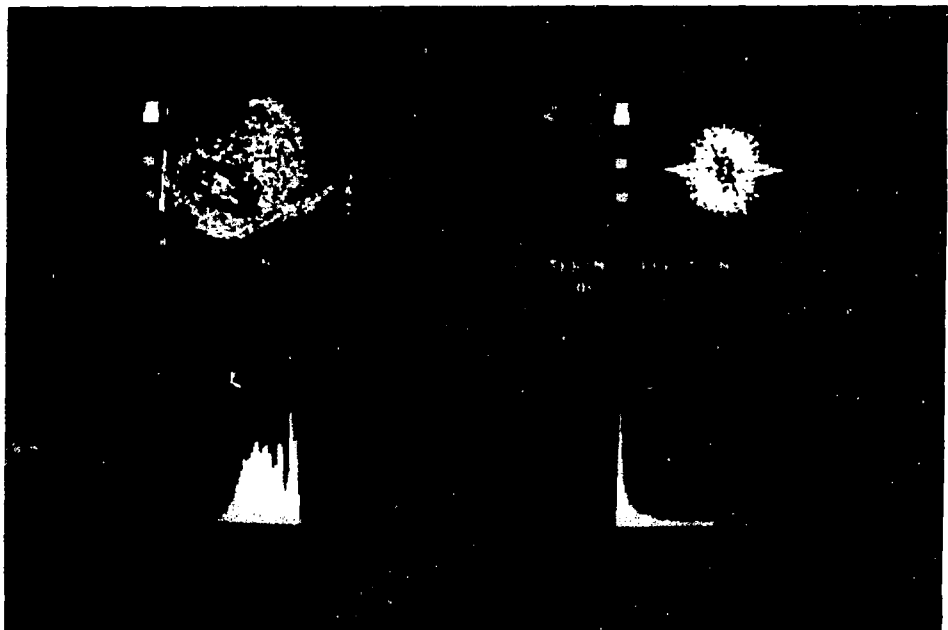3.5-d : Grey level histogram of Fig -b.

Fig 3.6-a: Raw image (Ultrasonic sector scan of Kidney recorded
           in 35mm film & digitized using densitometer of 8 bit
           resolution or 256 levels).
    3.6-b: Image obtained by Butterworth low pass filtering.
    3.6-c: Grey-level histogram of Fig -a.
    3.6-d: Grey level histogram of Fig -b.

revealed in the raw image.

Gaussian filter: This filter has monotonous response (without ringing). The response is maximum and symmetric about it's center frequency. Fig. 3.7 shows the one dimensional representation of a Gaussian filter. Two dimensional Gaussian filter is obtained by revolving the curve around the central axis. Such filters are depicted usually by plan views. Fig. 3.8(a) shows the input image and the Fig. 3.8(b) shows the transfer function of Gaussian filter. This is a spatial frequency domain representation (plan view of the convex dumb bell shape). Fig. 3.9 depicts the processed image after gaussian blurring. Fig. 3.10 depicts reverse operation of deblurring to obtain the original image. Fig. 3.11 depicts the effect of deblurring the image with known Fourier transform. As the operations are reversible, the images are restored to their original form, as can be seen by a comparison of Fig. 3.9(a) and 3.10(b).

Image compaction & Transform Coding:-

An image is represented as a set of data vectors which usually has highly correlated elements. When the image is transformed into another set of vectors, the size of the data vector determines the order & dimension of the transform. We know that a continuous "picture function" $f(x,y)$ can be represented by a set of orthogonal basis functions, for a bandlimited and highly over sampled picture.

Fig 3 6 a Raw image (Ultrasonic sector scan of kidney recorded in 35mm film & digitized using densitometer
         of 8 bit resolution or 256 levels)
     3 6 b Image obtained by Butterworth low pass filtering
     3 6 c Grey level histogram of Fig -a
     3 6 d Grey level histogram of Fig -b

Fig 3 7   Frequency characteristics of a Gaussian filter (one dimensional)
         Two dimensional filter is generated by revolving this curve through the
         centre frequency The plan view at two specific locations are shown as
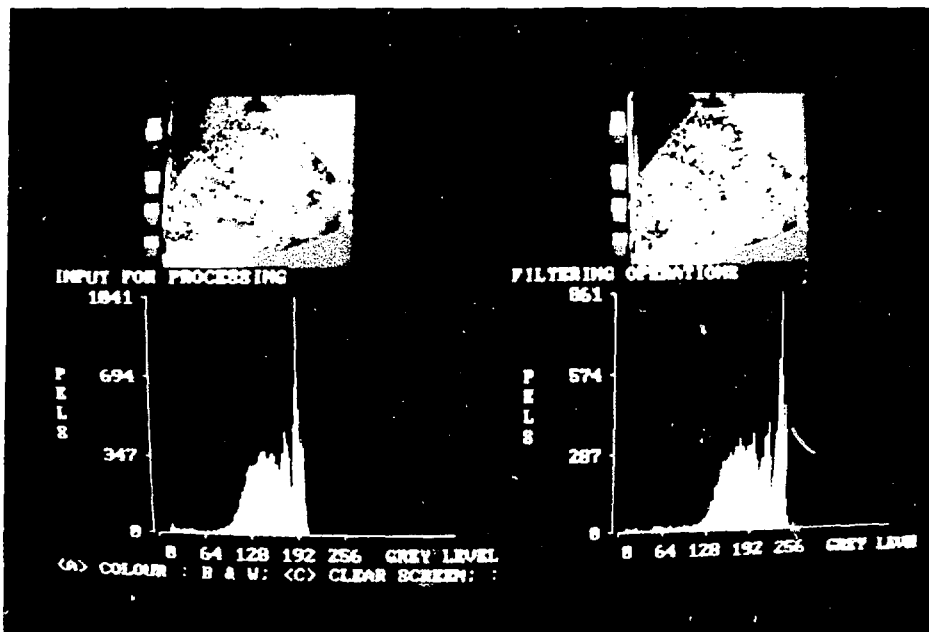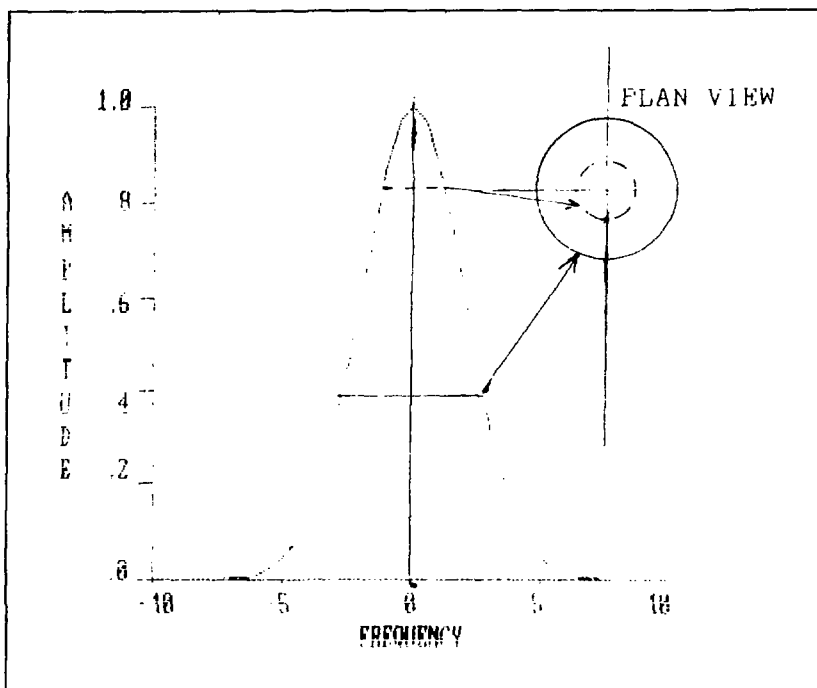   two circles of different dimensions

Fig. 3.8 a   Raw image (Ultrasonic sector scan of kidney recorded in 35mm film & digitized using densitometer
         of 8 bit resolution or 256 levels)
    3.8 b   2D view of transfer function of Gaussian filter
    3.8 c   Grey level histogram of Fig. a
    3.8 d   Grey level histogram of Fig. b

Fig. 3.9 a   Raw image (Ultrasonic sector scan of kidney recorded in 35mm film & digitized using densitometer
         of 8 bit resolution or 256 levels)
    3.9 b   Gaussian blurred image
    3.9 c   Grey level histogram of Fig. a
    3.9 d   Grey level histogram of Fig. b
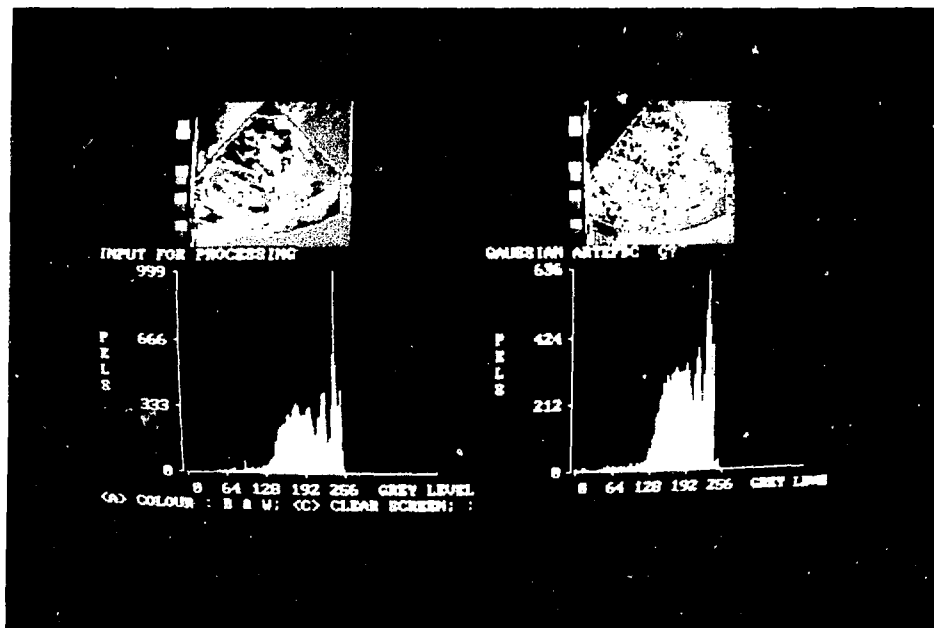
Fig. 3.10-a : Gaussian blurred image.
   3.10-b : Deblurred image. (Gaussian deblurring transfer function limited to near origin)
   3.10-c : Grey level histogram of Fig -a.
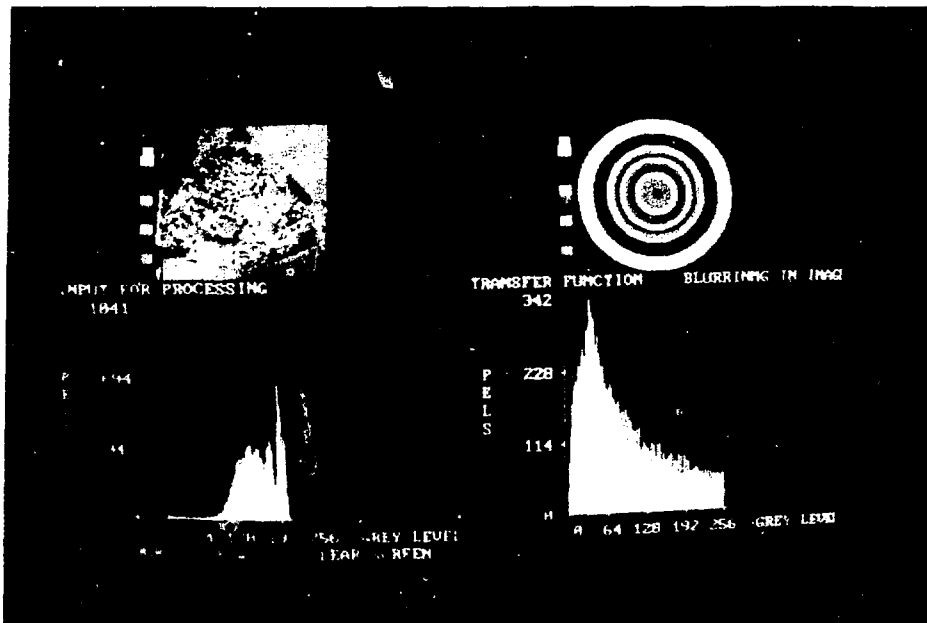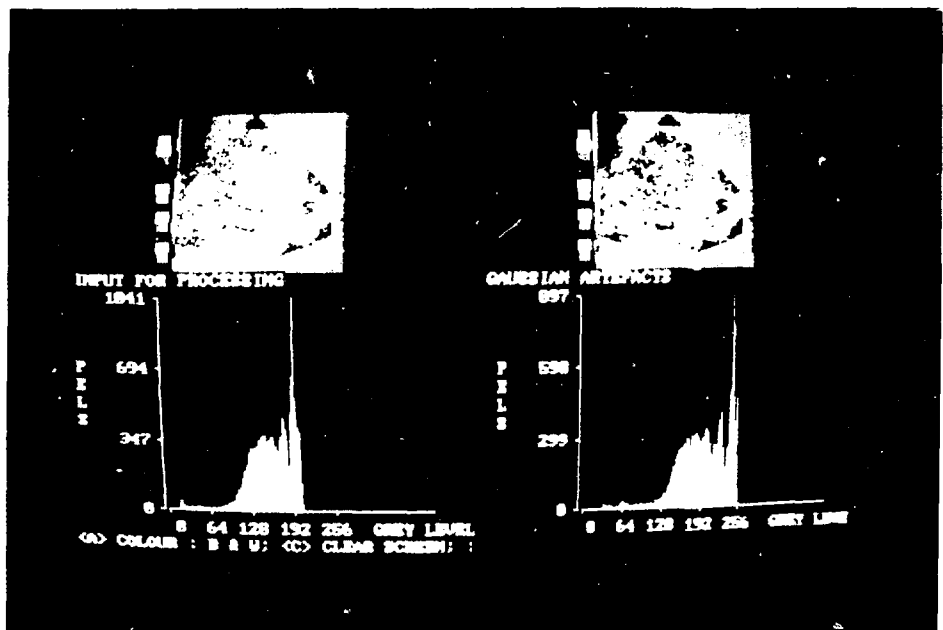   3.10-d : Grey level histogram of Fig -b.
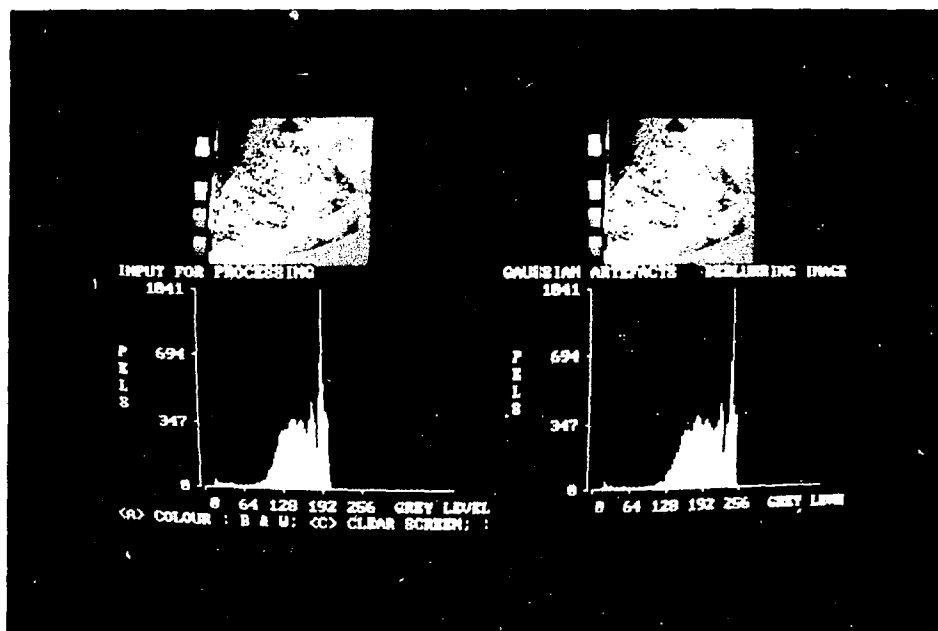
Fig 3.11-a : Raw image (Ultrasonic sector scan of kidney recorded in 35mm film & digitized using densitometer of 8 bit resolution or 256 levels).
   3.11-b : Image obtained by Gaussian deblurring with known Fourier Transforms
   3.11-c : Grey level histogram of Fig -a.
   3.11-d : Grey level histogram of Fig -b.

Orthogonal transforms are classified into two types. (i) Optimal transforms (ii) Sub optimal transforms.

The property of optimal transforms is reflected in its characteristics that it gives minimum errors in reconstruction. Such transformations result in a matrix of completely decorrelated elements. But the sub-optimal transforms do not decorrelate the data completely and gives rise to errors in reconstruction.

Image matrix contains redundant information and so it is possible to compact it, if optimum transforms are employed. Optimum transforms are those which could completely decorrelate pixel to pixel dependencies. All known transforms like fourier, Walsh, Hadamard, Haar & such transforms are sub-optimal transforms because the elements of transformed matrices are not fully decorrelated. They are partially decorrelated. The Karhunen-Loeve transform is the optimal transform because the covariance matrix for image block data is diagonalized leading to fully decorrelated K-L transform variables. (See Appendix 1 to 6 for details) Out of these the DFT is the transform involving complex transformation kernels and thus involve high computational timings for operations. Others require comparatively lesser timings & hence more suitable for on-line processing applications. K-L transforms being optimal reduces the Image data into a set of independent (uncorrelated) components. These components are generated from two parameters namely - mean

vector & co - variance matrix, and can be used to generate the image data with different and decreasing extent of errors.

GREY-LEVEL CO-OCCURRENCE, (MATCHED) TRANSFORM:In this transformation two images of the same object (taken by two sensors) are compared. As the images are identical, the two dimensional matrix [h] of grey level histogram will have non-zero values along the diagonal alone. Element h(i,j) represents the number of pixels with grey level i in picture 1 that have grey level j in picture 2. When the two pictures are not-identical, then [h] is no longer a diagonal matrix, but it has non diagonal entries. The matched transform tries to generate one picture obtained by linear representation of the [h] matrix. Karhunen-Loeve transform, (or principal component analyses, as it is also called) can be used to carry out this conversion to linear representation. The selection of the component with largest eigen value leads to the image with least errors as compared to the images obtained by any one of the other components. Fig.3.12 shows two images for the purpose of generating "matched transform" based image. Fig. 3.12(c) shows two dimensional grey-level co - occurrence histogram, which is a diagonal matrix. The reconstructed image based on "matched transform" operation is shown in Fig. 3.13(c). The image appears to be smoothed; however all edge - details are preserved.
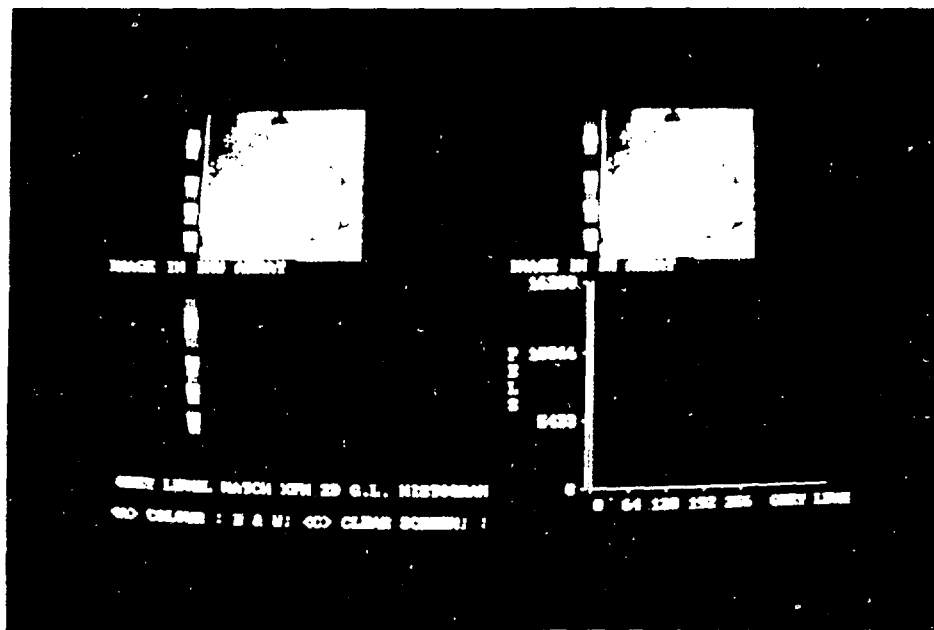
37
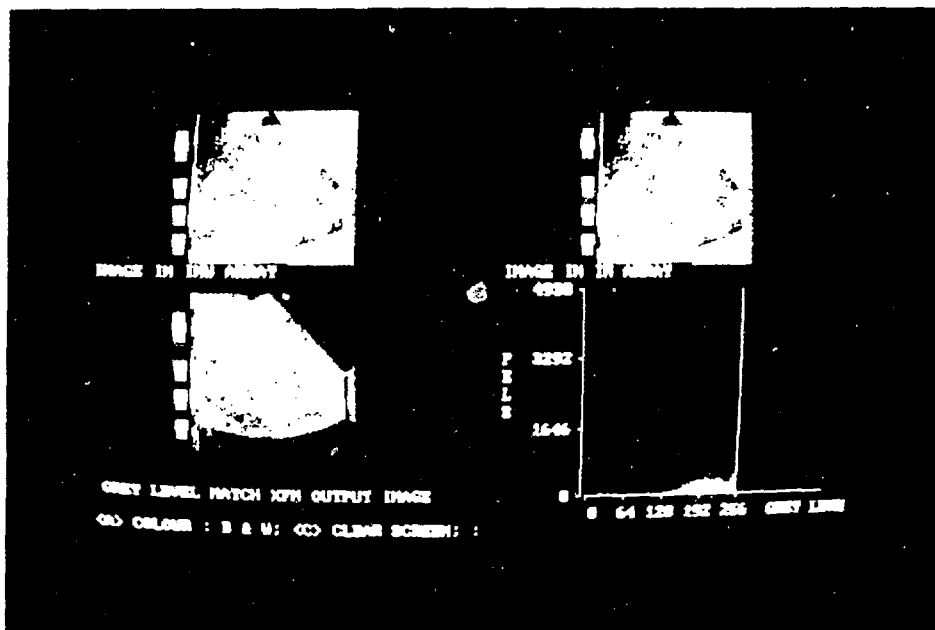
Walsh-Hadamard transform(WHT): This is a suboptimal orthogonal transform with square wave transformation functions. These are real valued functions unlike DFT which is a complex function. WHT is described by sequencies which is half the number of zero crossings in the interval (0,1). The WHT coefficients are called Sequency components. This transform is computationally fast because they involve only 1's and -1's. Figure 3.14 shows a geometrical figure a circle within a square. "W-H compacted image" is shown in Fig. 3.14(c). It is advantageous to use such transforms for coding & transmission. Fig. 3.15 shows model - input image - matrix (8x8) and the intensity levels are arbitrarily varied from 1 to 64. This image is used to check the transform routines.

Discrete Cosine Transform(DCT):This transform is similar to WHT, with the following dissimilarity. The basis vectors are sampled cosine functions and the transformation matrix is given as

$$H= 1/\sqrt{N} \ [H_{kl}]$$

$$\text{where } H_{kl} = \begin{cases} 1, & l = 0 \\ \\ \sqrt{2}\cos[(2k+1)l\Pi/2N] & k = 0,1,2....N-1 \\ & l = 1,2,.....N-1 \end{cases}$$

The computation algorithm is made fast using FFT algorithms for 2N points. DCT is slow but efficient computationally because
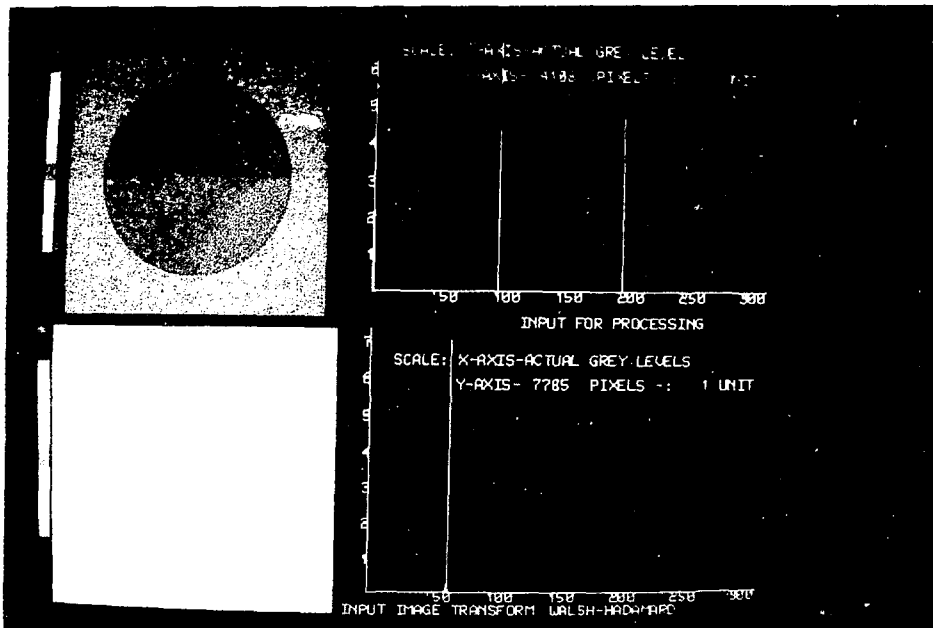
Fig 3 14 a Modified geometric object a square containing a circle
     3 14 b Grey level histogram of Fig a
     3 14 c Walsh Hadamard transform of image a
     3 14 d Grey level histogram of Fig c

1	2	3	4	5	6	7	8
9	10	11	12	13	14	15	16
17	18	19	20	21	22	23	24
25	26	27	28	29	30	31	32
33	34	35	36	37	38	39	40
41	42	43	44	45	46	47	48
49	50	51	52	53	54	55	56
57	58	59	60	61	62	63	64

Fig 3 15 Sample input image 8 '8 pixels used for checking transform routines

the forward and the inverse transformation kernels turn out to be the same. Fig. 3.16 gives DCT of image data shown in Fig. 3.15. It can be seen that only the first row & first column carry the transformed / coded information of the image data; also that the third, fifth and seventh rows & columns are all zero. Thus, data compaction is very large indeed.

Haar Transform: This transform has elements 1, -1, 0 and powers of $\sqrt{2}$. The first coefficient is the mean of the vector, the second is the difference of means between first half and the second half elements of the vector. The remaining coefficients in groups of power of two (2^k, k=1,2,3,4...,n-1) are weighted (weight equal to $[\sqrt{2}]^k$) difference of means of the vector elements at different positions of the vector and the element count for averaging is given as 2^l, l=n-2,n-3,...,1,0. For example when the vector is of 4 elements, the third coefficient is the difference of first two elements weighted by $\sqrt{2}$ and the fourth element is similarly weighted difference of third and fourth element. It can be verified easily that Haar transform of N element vector involves N(n+1) additions and $2+2^1+2^2+...+2^{n-1}$ multiplications.

The Haar transform is both globally and locally sensitive as it involves parts of the vector for computation of third and subsequent coefficients of the transform. Fig. 3.17 gives HT of image data shown in Fig. 3.15. It can be seen that only the first row and the first column carry the transformed / coded

41

```
260.00 -145.77    0.00  -15.24    0.00   -4.55    0.00   -1.15
-18.22    0.00    0.00    0.00    0.00    0.00    0.00    0.00
  0.00    0.00    0.00    0.00    0.00    0.00    0.00    0.00
 -1.91    0.00    0.00    0.00    0.00    0.00    0.00    0.00
  0.00    0.00    0.00    0.00    0.00    0.00    0.00    0.00
 -0.57    0.00    0.00    0.00    0.00    0.00    0.00    0.00
  0.00    0.00    0.00    0.00    0.00    0.00    0.00    0.00
 -0.14    0.00    0.00    0.00    0.00    0.00    0.00    0.00
```

Fig 3.16: Discrete cosine transform of image data shown
          in Fig 3.15.

```
 32.50   -2.00   -0.71   -0.71   -0.25   -0.25   -0.25   -0.25
-16.00    0.00    0.00    0.00    0.00    0.00    0.00    0.00
 -5.66    0.00    0.00    0.00    0.00    0.00    0.00    0.00
 -5.66    0.00    0.00    0.00    0.00    0.00    0.00    0.00
 -2.00    0.00    0.00    0.00    0.00    0.00    0.00    0.00
 -2.00    0.00    0.00    0.00    0.00    0.00    0.00    0.00
 -2.00    0.00    0.00    0.00    0.00    0.00    0.00    0.00
 -2.00    0.00    0.00    0.00    0.00    0.00    0.00    0.00
```

Fig 3.17: Haar transform of image data shown in Fig 3.15.

information of the image data: and that because of repeatability in the transformed elements, compaction of the image data is achieved, to a large extent.

Slant transform: The Slant transform is another fast, sub ptimal, orthogonal transform, which uses sawtooth waves in place f sinusoids or step functions for fitting the input data, leading to the transfor .d output image. See Fig.3.18 for the coded image representation corresp :ding to input image shown in Fig. 3.15. It can be seen that except for th first & the second elements in the first & second row and column, all other values are zero: thus reducing the image to a three number - representation in place of 64.

Hartley Transform: It is an orthogonal sub optimal transform which has a real valued kernel. As before except the first row & column all other values are zero. Only 14 numbers are required to represent 64 element image.

Hartley transform is quite similar to the DFT, but has no complex terms and therefore it is quite fast and efficient. It can be computed using the FFT also. The advantages of Hartley transform over FFT for real data are 1) it requires only half the array space, 2) it has identical forward and inverse transforms, 3) it is a direct conversion to power spectral density function. See Fig. 3.19 for coded image representation corresponding to input image shown in Fig. 3.15.

```
260.00   -18.37    0.00    0.00    0.00    0.00    0.00    0.00
-146.64    0.00    0.00    0.00    0.00    0.00    0.00    0.00
   0.00    0.00    0.00    0.00    0.00    0.00    0.00    0.00
   0.00    0.00    0.00    0.00    0.00    0.00    0.00    0.00
   0.00    0.00    0.00    0.00    0.00    0.00    0.00    0.00
   0.00    0.00    0.00    0.00    0.00    0.00    0.00    0.00
   0.00    0.00    0.00    0.00    0.00    0.00    0.00    0.00
   0.00    0.00    0.00    0.00    0.00    0.00    0.00    0.00
```

Fig 3.18: Slant transform of image data shown in Fig 3.15.

```
 32.50    -1.71   -1.00   -0.71   -0.50   -0.30    0.00    0.71
-13.66     0.00    0.00    0.00    0.00    0.00    0.00    0.00
 -8.00     0.00    0.00    0.00    0.00    0.00    0.00    0.00
 -5.66     0.00    0.00    0.00    0.00    0.00    0.00    0.00
 -4.00     0.00    0.00    0.00    0.00    0.00    0.00    0.00
 -2.34     0.00    0.00    0.00    0.00    0.00    0.00    0.00
  0.00     0.00    0.00    0.00    0.00    0.00    0.00    0.00
  5.66     0.00    0.00    0.00    0.00    0.00    0.00    0.00
```

Fig 3.19: Hartley transform of image data shown in Fig 3.15.

In essence, all transform domain operations generate either correlated or uncorrelated variables. The transformed matrices are then ordered (or arranged in some sequence) and denoted using the principles of matrix rendition. Such a step provides elegance to the whole approach and a possibility to encode image informations for possible applications like "on-line" Processing, Compaction, image transmission, etc.

The inverse operations recognize degradative processes involved in the sequence of imaging and provide a technique to recover information lost in the sequence of operations. It is here that Wiener's principle of minimum mean - square error (MMSE) plays a dominant role, although the problem is reckoned from the statistical view points. Thus statistical communication theory becomes the hallmark for progress in our understanding.

Wiener - Khinchine's theorem namely "Auto correlation and Power Spectrum are Fourier transform pairs" provides an experimental technique to link the Statistical & the Engineering approaches: And it is only proper that K-L transform adopts statistical parameters like the covariance matrices for generating fully decorrelated variables which finds various applications in Image processing, proper registration of satellite images, template matching, etc.

IV. SPATIAL WINDOW PROCESSING (NEIGHBOURHOOD OPERATIONS)

A moving window of size (n x m) is subjected to many image processing operations. Neighbourhood processing as the operation is also called, involves operations on N x M pixels. Low pass filtering operations such as local averaging (both recursive & non-recursive), Jong-Sen filtering (k < 1), median filtering, percentile filtering, maxmin / minmax filtering, are employed to smoothen the appearance of the image. High pass filtering such as laplacian filtering, Jong-sen filtering (k > 1), and image shift-filter are employed to enhance edge details in images. Kuwahara filtering is a low pass statistical filter which does not "smear" the edge information because of the folding type of operations, unlike the trapezoidal filter.

Neighbourhood processing, as above, are dependent on the surrounding pixel values. These operations thus involve convolution kernels. These kernels are specific to different types of the filtering employed. There are two types of filtering operations generally employed in image processing . They are non-recursive & recursive filtering. In non-recursive filtering, as in say local averaging , the value of all the pixels inside the window is substituted by the average value (of groups of pixels within the window). The window is moved by one window size to the right & the process is repeated, till the entire area of the image is scanned. In this way, abruptness in the pixel data is smoothened and uniformity in the picture is introduced. It can be

46

inferred that 9 x 9 window will smoothen the image better than 3 x 3 window. The average values computed in the previous operation have no bearing on the future operations & hence the operations is said to be non-recursive. Fig. 4.1 illustrate the effect of non – recursive window operation carried out on the raw image. It can be seen that the pixel values have also been altered giving an overall effect to the global nature of the image.

In recursive window operations, the average value computed for one window is assigned to the central pixel and the window is shifted by only one pixel to the right. In the actual computation scheme, the sum of pixel-values for one column of pixel to the left of the window is replaced by that for the next column when the window-average for the second position is computed and this sequence is repeated till the entire area is scanned. It can be seen that the computational scheme takes advantage of the previous calculations and thus the process becomes recursive. In general the past value will have its bearing on the values presently computed. Such operations are called recursive filtering.

Jong-Sen filtering: This is a window filter which not only takes into account the window mean, but also a factor K of deviations in pixel values from the mean for computing the output value. Therefore the constant multiplier K can be varied to obtain high pass as well as low pass filtering. For values of

Fig. 4.1 appears on page 50 alongwith Fig. 4.2.

Fig 4.1-a: Raw image (Ultrasonic sector scan of Kidney recorded
in 35mm film & digitized using densitometer of 8 bit
resolution or 256 levels).
4.1-b: Image obtained by non-recursive window (3x3)
averaging.
4.1-c: Grey-level histogram of Fig -a.
4.1-d: Grey level histogram of Fig -b.

K < 1, it acts as a low pass filter and for K > 1, it acts as a high pass filter.

Window averaging operations with N points window, produces an improvement of √N in the SNR. The convolution kernel for local averaging with 3 x 3 window is given by

$$\begin{bmatrix} 1/9 & 1/9 & 1/9 \\ 1/9 & 1/9 & 1/9 \\ 1/9 & 1/9 & 1/9 \end{bmatrix}$$

and it can easily be seen that the information /details will be average´.

Kuwahara Statistical Filtering: It is a statistical filter which estimates parameters like mean and variance of four overlapping quadrants of a window with a common pixel in the picture. The mean of the window corresponding to the minimum variance is chosen and put for the common pixel. This smoothing operation also preserves the edges information.

Kuwahara filtering is superior to any other low pass filter (even better than the median filter that has better edge preservation as compared to window averaging) to a large extent. The window size here should also be chosen with care, taking into account noise effects and artifacts. In Fig. 4.2, a noisy geometrical object is subjected to Kuwahara filtering of (5x5) window. It can be seen that the processed image is superior even
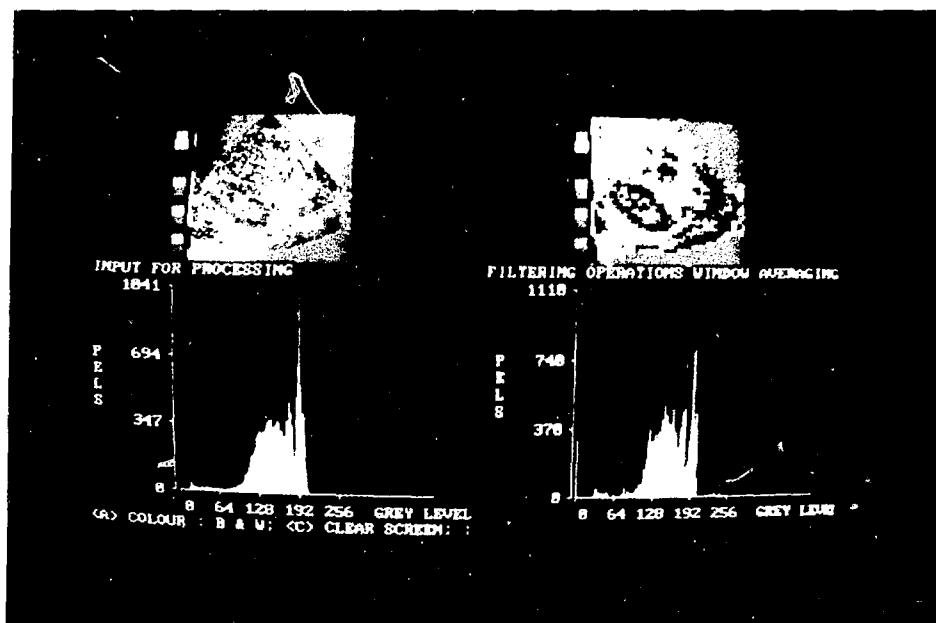
49

Fig 4 1 a Raw image (Ultrasonic sector scan of kidney recorded in 35mm film & digitized using densitometer
           of 8 bit resolution or 256 levels)
    4 1 b Image obtained by non recursive window (3x3) averaging
    4 1 c Grey level histogram of Fig a
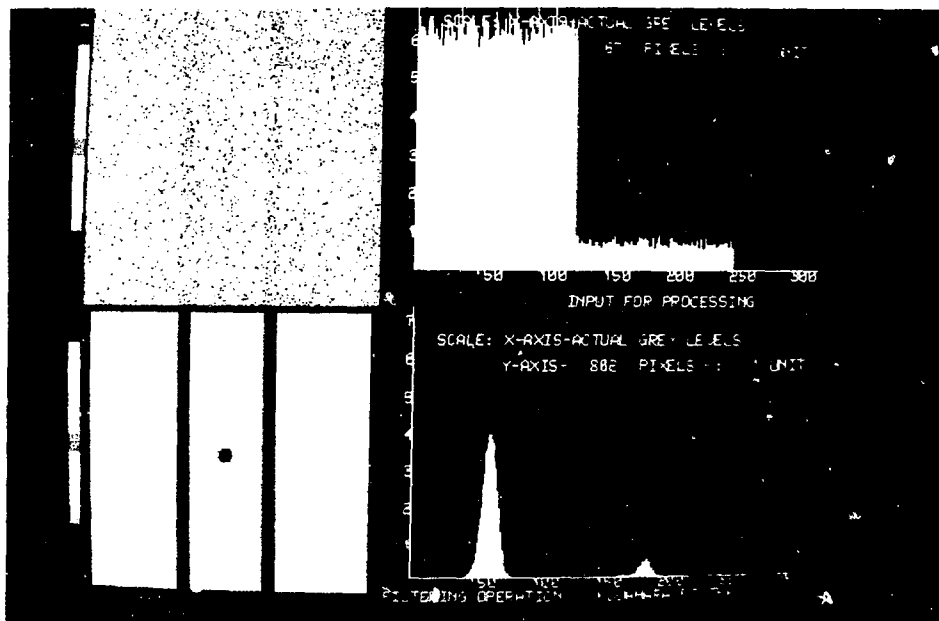   4 1 d Grey level histogram of Fig b

Fig 4 2 a Modeled image of a noisy geometrical objects using ND 560 system
    4 2 b Grey level histogram of Fig a
    4 2 c Image obtained by Kuwahara 13x13 window filter
    4 2 d Grey level histogram of Fig b

to trapezoidal filtering (Fig. 3.3) in that the edge details ar-

preserved. Such an advantage ensues in view of the fact that the

edges are not smeared as in window averaging because of folding

operations involved. Fig. 4.3 refers to the kidney raw image and

the processed image. The effect of Kuwahara filtering in

preserving the geometric details can again be discerned.

Maxmin Filtering: It operates on the maximum and the minimum

pixel values, computed for the window. The central pixel is

replaced by the minimum pixel value. This is then followed by

computation of maximum pixel value and substitution. The entire

sequence is recursively executed. Such operations secure noise

removal in image processing applications. This filter is said to

remove white objects on black backgrounds.

Minmax filtering: Here the operations are similar to that of

maxmin filter but in reverse sequence. Consequently, this filter

eliminates black objects on white background.

Shift And Subtract Filtering: Here the input image is shifted

and subtracted from the original image. The image so obtained

will highlight edge-details prominently. The grey level could be

stretched to occupy 0-255 levels, to reveal further hidden

details.

The shift can be done in the X, Y, or XY directions,

respectively depending on whether the the edge is in the X, Y, or

Fig. 4.3 appears on page 54 alongwith Fig. 4.4.

Fig 4.3-a: Raw image(Ultrasonic sector scan of Kidney recorded in 35mm film & digitized using densitometer of 8 bit resolution or 256 levels).
4.3-b: Image obtained by Kuwahara (5x5) window filtering.
4.3-c Grey-level histogram of Fig -a.
4.3-d: Grey level histogram of Fig -b.

XY direction. The shift depicts the thickness of the edge, whereas the threshold shows the grey level region of our interest. Fig. 4.4(a) shows the image when subjected to shift and subtract operation, shift being in X direction. As the result of subtraction can be both positive and negative, the zero (dc) value in the resultant image shifts to mid scale psuedocolour (green as is evident from the scale in Fig. 4.4). From Fig. 4.4(b), it can be seen that low spatial frequencies have been removed and the vertical regions of the contours are enhanced.

Digital Laplacian : Laplacian operator sharpens picture details and removes blur.

Laplacian filtering in the digital form can be described by the relation.

$$\{ 4f(i,j) - [f(i+1,j)+f(i-1,j)+f(i,j-1)+f(i,j+1)] \}$$

where the pixel values are shown in graphical form, as below.

For keeping the magnitude within the fixed word length the following form is used

$$\{ f(i,j) - 1/4 [f(i+1,j)+f(i-1,j)+f(i,j-1)+f(i,j+1)] \}$$

The convolution kernel for the Laplacian filter can be given as

$$
\begin{bmatrix}
 & -1/4 & \\
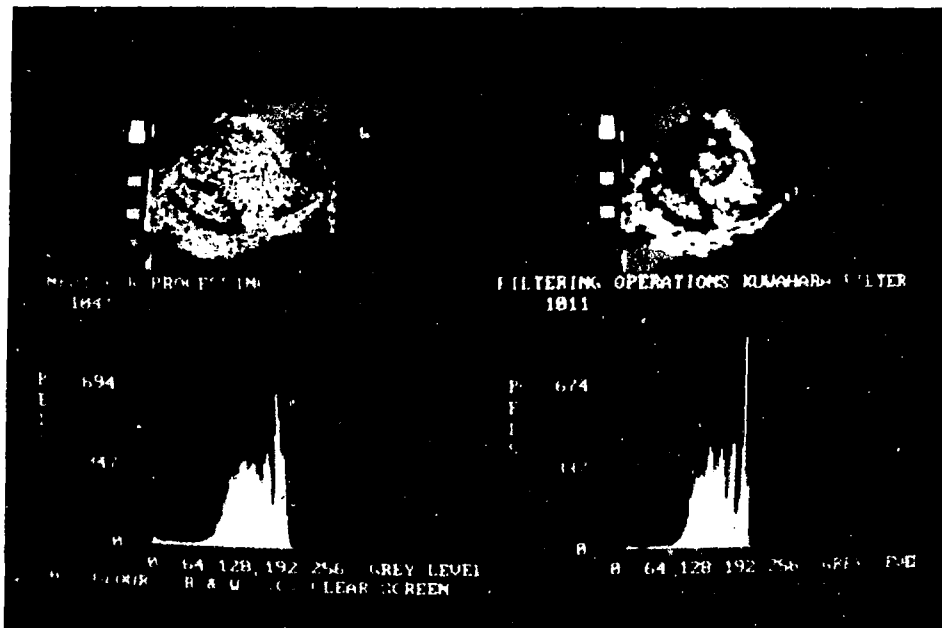-1/4 & 1 & -1/4 \\
 & -1/4 &
\end{bmatrix}
$$

Fig .4.3-a : Raw image (Ultrasonic sector scan of kidney recorded in 35mm film & digitized using densitometer of 8 bit resolution or 256 levels).

4.3-b : Image obtained by Kuwahara (5x5) window filtering.

4.3-c : Grey level histogram of of Fig -a
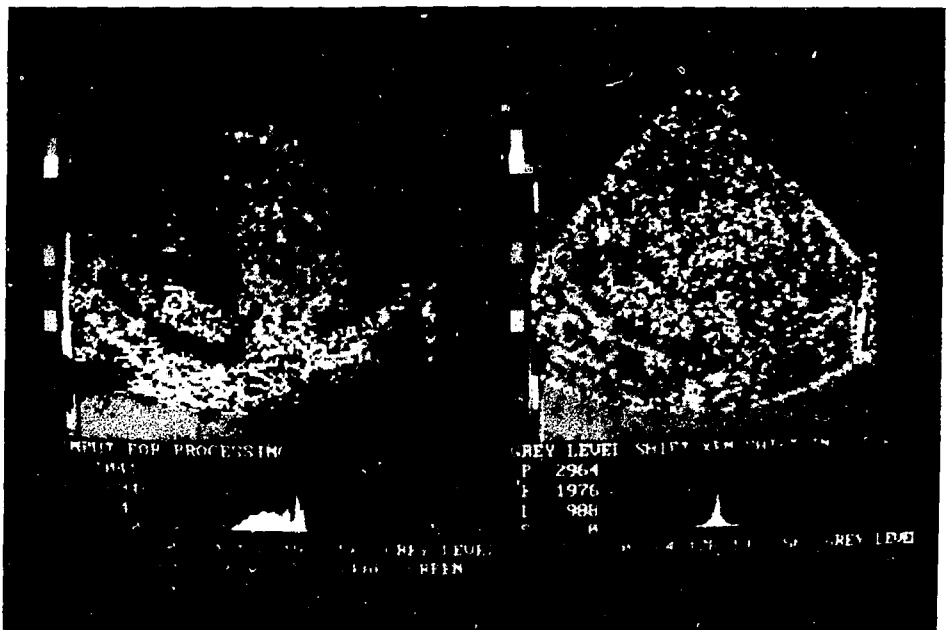
4.3-d : Grey level histogram of Fig -b.

Fig 4 4 a   Raw image (Ultrasonic sector scan of kidney recorded in 35mm film & digitized using densitometer of 8 bit resolution or 256 levels)

4 4 b : Image obtained by x shift & subtract on Fig a Both a & b have been magnified to 256x256 pixels

4 4 c   Grey level histogram of Fig -a

4 4 d   Grey level histogram of Fig -b

As in the shift and subtract operation, the output can be either stretched to occupy full grey level range for high frequency emphasis or converted to binary picture based on the user specified threshold. The pixel is set to 1 if the threshold is crossed or else it is set to 0. The Laplacian can be combined (a fractional value added) to the original picture to obtain edge - enhanced picture. A modeled image (see Fig.4.5) is subjected to Laplacian filtering with a threshold of 20. (b) is the processed image where only edge details are preserved & highlighted. As shown earlier, (c) & (d) refers to GL distribution for (a) & (b) respectively. It can be seen that Laplacian operator is useful for edge detection, contouring, edge-enhancement, etc.

TEMPLATE MATCHING: In template matching, a small image representing a template is moved over all possible positions of a large image that is likely to contain the template. In our case the template image consists of a square of side 220 pixels long with grey level value = 100. A circle of radius 80 pixels and grey level of 200 is included in the square. This symmetric object template is matched with the image having same size and grey-levels. The template is moved around the image by 9 pixels in x and y directions leading to a matrix of 9x9 size.

In our discussion, first we shall consider case where the size of the template and that of the image are identical and they differ only in clarity. We shall compute cross-correlation

Fig 4.5-a: A noisy image of geometrical objects.
    4.5-b: Laplace edge detection with a threshold of 20 on -a.
    4.5-c: Grey-level histogram of Fig -a.
    4.5-d: Grey level histogram of Fig -b.

coefficients between the template and the "underlying image part" for every position. For a perfect match, the correlation coefficients will have the maximum value lying on the apex of a cone. This situation is similar to the computation of one dimensional correlation function, which is similar to that shown in Fig.4.6.

Fig 4.6 depicts the results of spline analyses.(performed on the x & y profiles through the apex of correlation matrix). For the sake of discussions the left half(A) of Fig.4.6 depicts "effects of noise" with no difference between the template and the Image. As we proceed along the column SNR is increased from 0 db to 100 db. The correlation coefficients vary from 1.0 to 0.910 respectively. These figures are the same for both X and Y profiles for equal displacements of pixels, in one direction.

It can therefore be concluded that when the template and the image are identical in size, the presence of even 100 db noise can pick out buried similarities, between a given template & its replica in the image.

Similarly, the right half(B) of Fig.4.6 depicts the situation when the template & the replica inside a given image differs in size by 2,4 6 pixels and the SNR in both are the same, with no noise conditions. It can be seen that the correlation coefficients vary from 0.980 - 0.945 for equal displacement of pixels, in one direction.
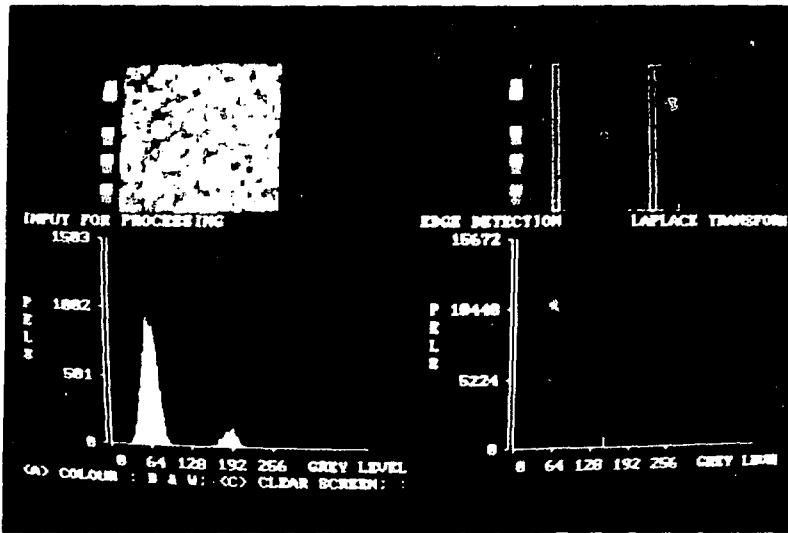
Fig 4.5 a A noisy image of geometrical objects
    4.5 b Laplace edge detection with a threshold of 20 on a
    4.5 c Grey level histogram of Fig a
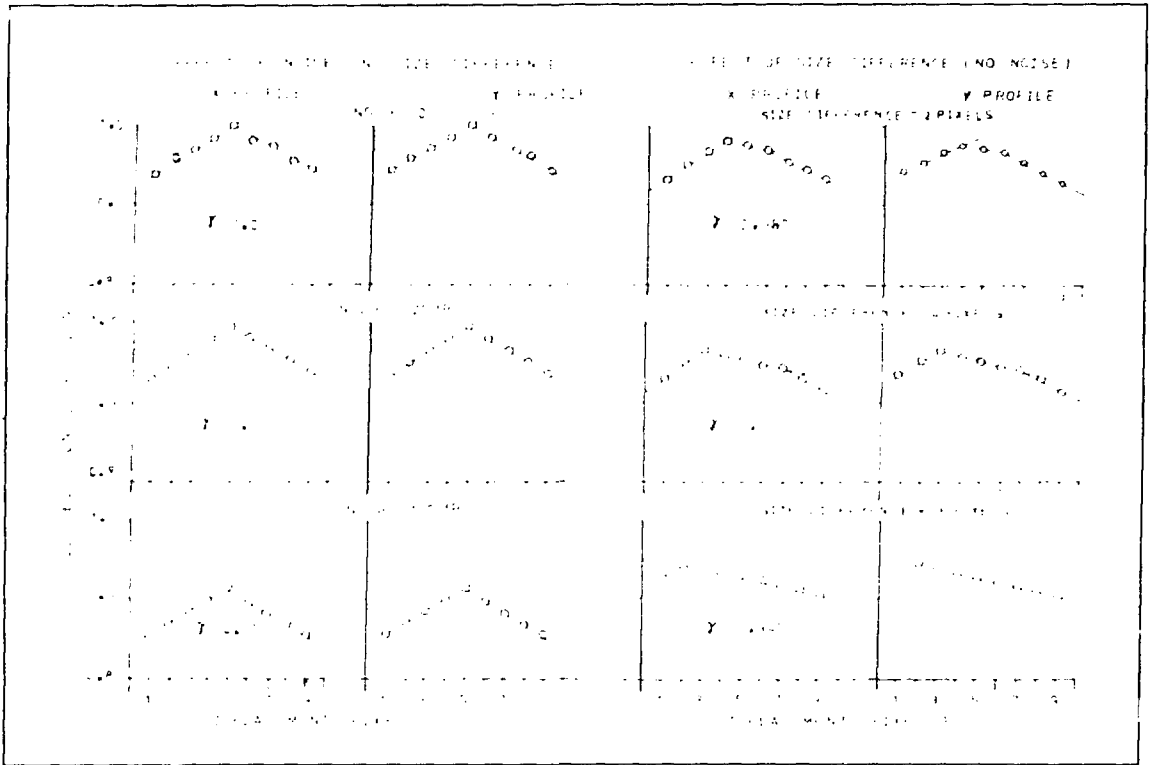   4.5 d Grey level histogram of Fig b

Fig 4.6   Graphical representation of correlation between 2 images (Template vs image)

It can therefore be concluded that even when the template &
its replica buried in the image differ by 2,4, or 6 pixel
dimensions, it is possible to identify buried templates in
Images.

When the size difference exists, the profiles can be fitted
with three splines, the central spline-length yields, in pixel
units, the difference between the image and the template (both
vertical and horizontal profiles can be considered). The length
of the central - spline is indicative of the degree of size
mismatch. The outer splines must be of opposite slopes and the
correlation coefficient at the apex must be significant. Degree
of mismatch is indicated by the deviation of apex correlation
coefficient from unity. Presence of more than three splines, in
either profile is indicative of no matching.

Thus using product moment correlation coefficients, inference
on "size differences" and "existence of template" can be made.

To sum up, a spatial window with suitable Kernel is convolved
with image data to locally alter the grey level distributions
within the window. It can be seen that the window operations are
easier to implement and statistical parameters are invariably
used to eliminate noise, or to extract hidden details or to
emphasize boundaries or to delineate geographic ground details
(as in satellite imaging) or for engineering applications as
template matching. It should be emphasized that all the

operations are well defined mathematically & are invertible and thus constitute potentially useful techniques to reveal hidden information.

V IMAGE ANALYSIS

Image analyses involves conversion of grey level Images into binary or two level images. It is also called grey level window operations. When a 64 - level Image information is to be converted into a binary image, the choice of the window is decided by the threshold setting of the operator. (It may be parenthetically remarked that such an operation makes the analysis subjective and hence adequate care has to be exercised for reliable analysis). Binary analysis aims at feature extraction and characterization. The resultant binary images often have artifacts, noise, etc., requiring "cleaning up operations". Logical operations such as AND, OR, XOR and NEGATE are used in association with dilation, erosion etc., in the cleaning up operations. Such operations are employed to select specified or interested regions in the raw image.

A Scanning Electron Microscope(SEM) image was digitized & "imaged" using the Video Frame Processor developed by our associate - groups in this section. The digital frame of Image stored in the system was transferred to IBM PC-AT system for further analysis.

Fig 5.1 shows the grey level image & the binary converted (180 - 243) image. Pseudocolouring of grey level image is used to highlight the composite nature of grain size distribution. The program enables display of both images as well as the
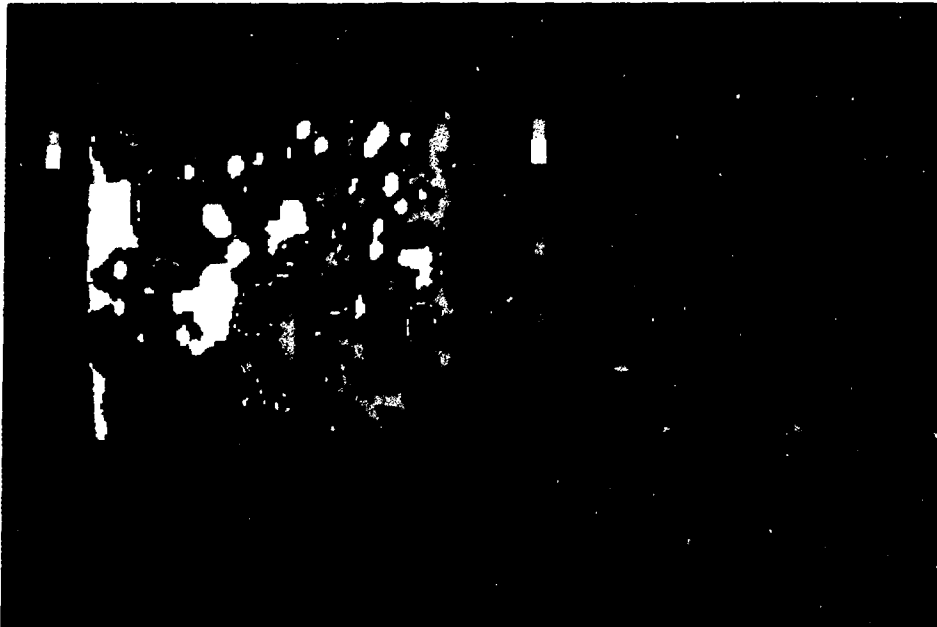
Fig. 5.1-a : Image data acquired with frame grabber from a SEM photograph of a metallurgical sample. The image is magnified to 256x256.

5.2-b : Grey level thresholded (180-243) binary image. The image is magnified to 256x256.

distribution of parameters measured on individual objects.

In Fig. 5.2, the objects touching the borders have been eliminated. Fig. 5.3 shows binary image obtained by close holes operation on the binary image shown in Fig. 5.2(b). To eliminate smaller objects of erosion size 2, the binary image is eroded twice (Fig. 5.3). Fig. 5.4 shows reconstructed image of Fig. 5.3(b) with the source image obtained from Fig. 5.2(b) after close hole operation.

Fig. 5.5 depicts the image after "fermeture " operation on the binary image shown in Fig. 5.4. This operation is useful in the reconstruction of broken grain boundaries in metallurgical samples. Fig. 5.6 depicts the image after "skeletonisation" of the image shown in Fig. 5.5. This operation is useful in characterizing the shape of objects, particularly details of chromosomal features involving the location of centromere. Fig. 5.7 depicts the "selection of objects" with a graphic cursor (black and white display of the same is shown in Fig. 5.8). Selected object and its features like projection, area, perimeter etc. are shown in Fig. 5.9.

To sum up, it can be seen that the binary image analysis can be used to obtain quantitative information. The given image is segmented into binary image to get the objects of interest delineated from unwanted noise and other artifacts. The

Fig. 5.2 a Image data acquired with frame-grabber from a SEM photograph of a metallurgical sample.
     5.2 b Grey level thresholded (180-243) binary image has been processed to remove objects on border
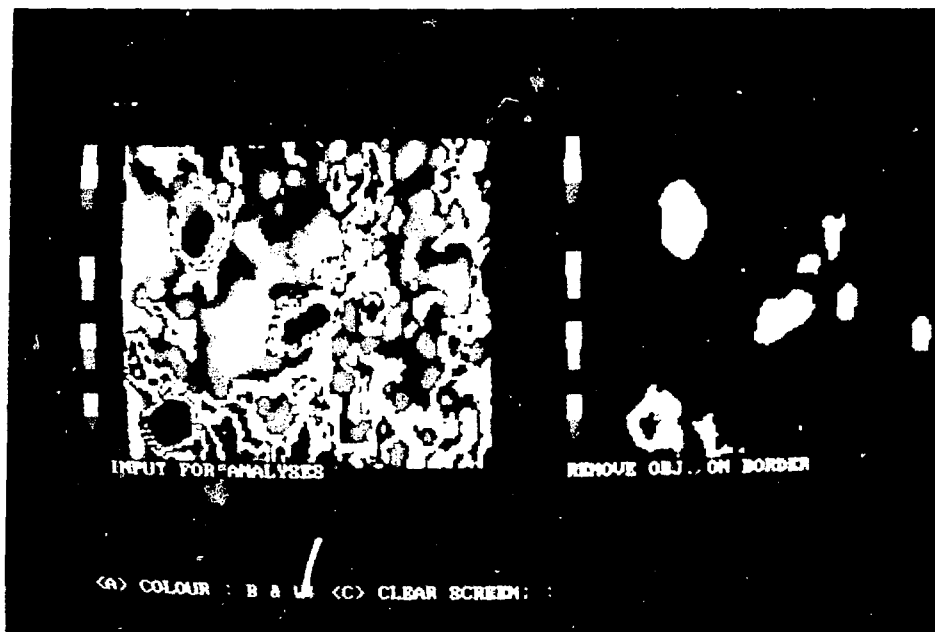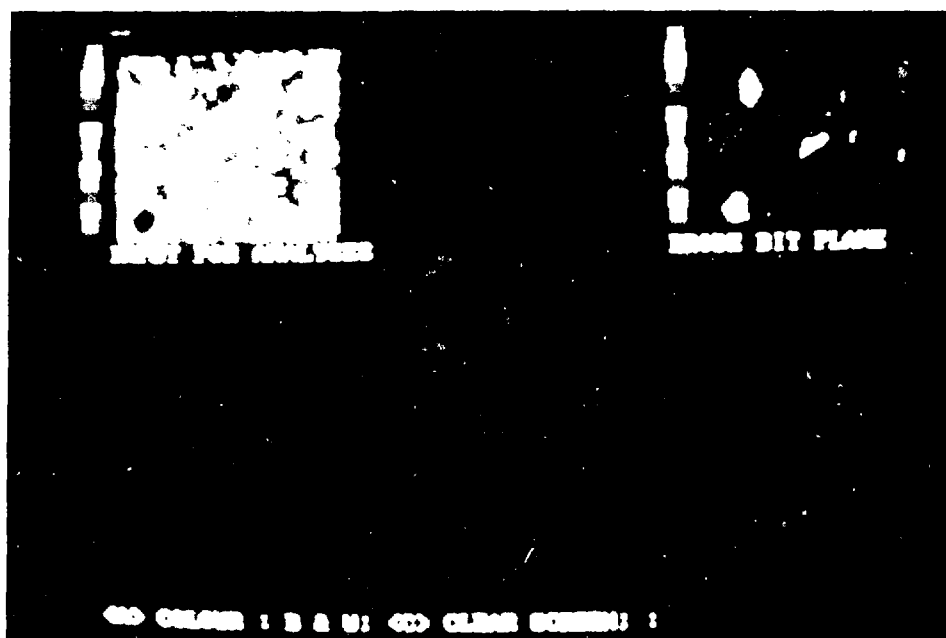

Fig. 5.3 a Image data acquired with frame-grabber from a SEM photograph of a metallurgical sample.
     (128 x 128)
     5.3 b Grey level thresholded (180-243) binary image has been subjected to erosion, with a 3 x 3 window, in one operation, further shrinking the objects by a 1 pixel removal on the boundary

Fig. 5.4-a : Image data acquired with frame grabber from a SEM photograph of a metallurgical sample (128 x 128)

5.4-b : Binary image obtained in Fig 5.3-b is reconstructed (dilation & logical AND) to restore the objects to the original size.
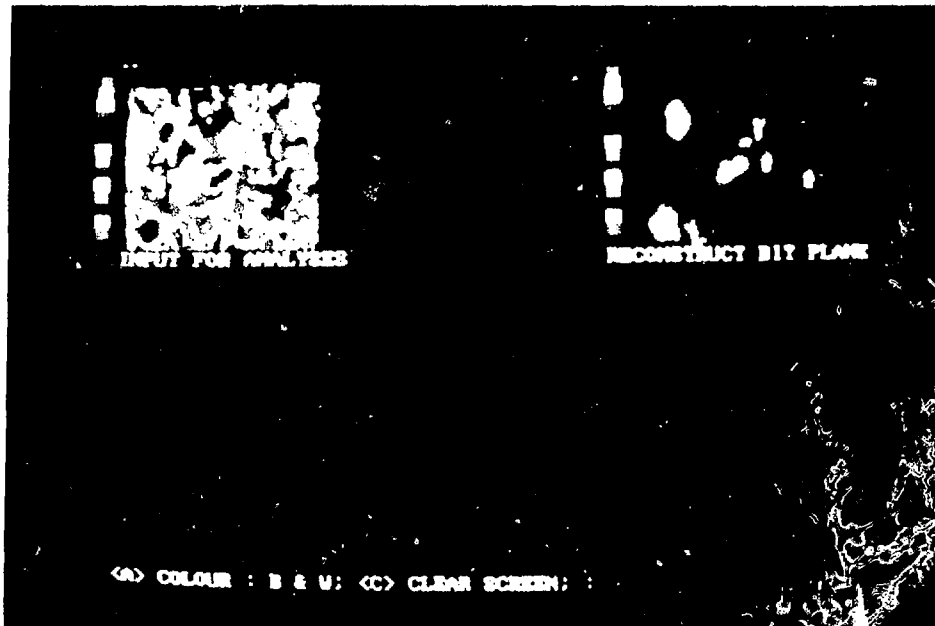

Fig. 5.5.a : Image data acquired with frame grabber from a SEM photograph of a metallurgical sample (128 x 128)

5.5.b : Binary image obtained in Fig. 6.4-b is subjected to fermeture operation of order 3 (3 dilations followed by 3 erosions). Notice the merging of close by objects

Fig 5.6 a Image data acquired with frame grabber from a SEM photograph of a metallurgical sample (128 x 128)
5.6 b Binary image of Fig 5.5 (b) is skeletonised
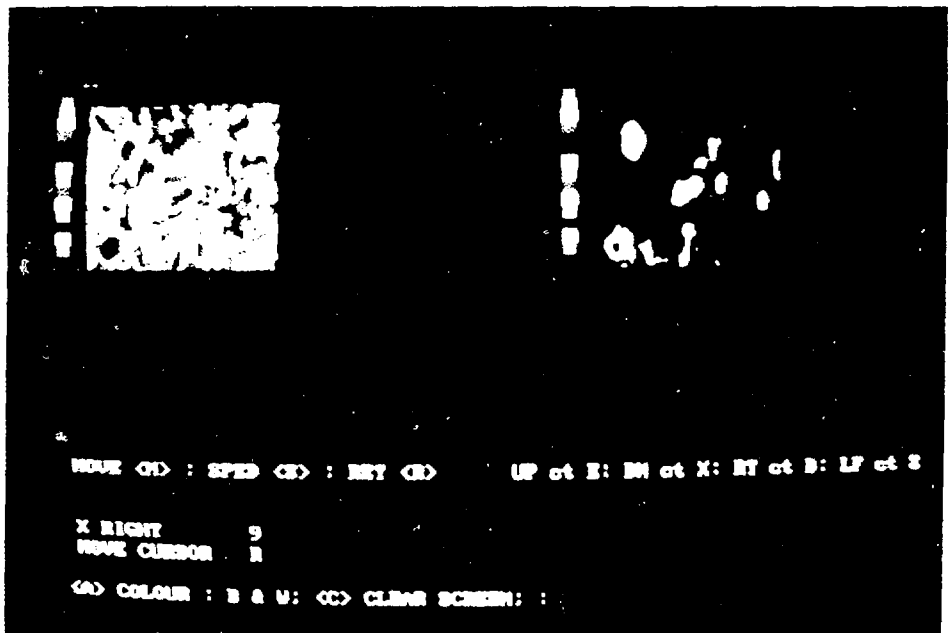
Fig 5.7 a Image data acquired with frame grabber from a SEM photograph of a metallurgical sample (128 x 128)
5.7 b Binary image obtained by grey level window (185, 245) preprocessed to select objects with a graphic cursor

Fig 5 8 a Image data acquired with frame grabber from a SEM photograph of a metallurgical sample
(128 ×128)
5 8 b Binary image obtained by grey level window (180-243) is processed to select object with a graphic
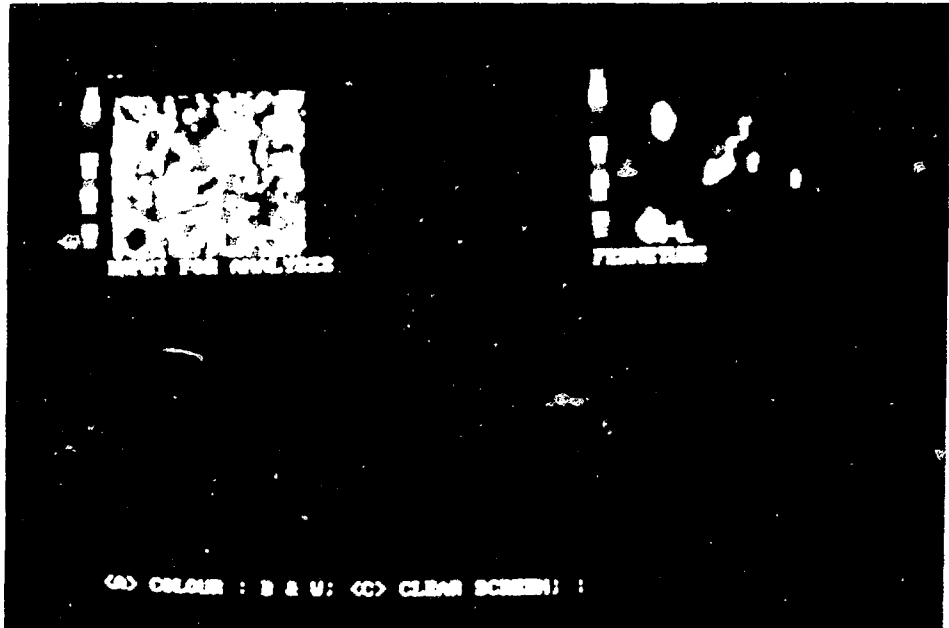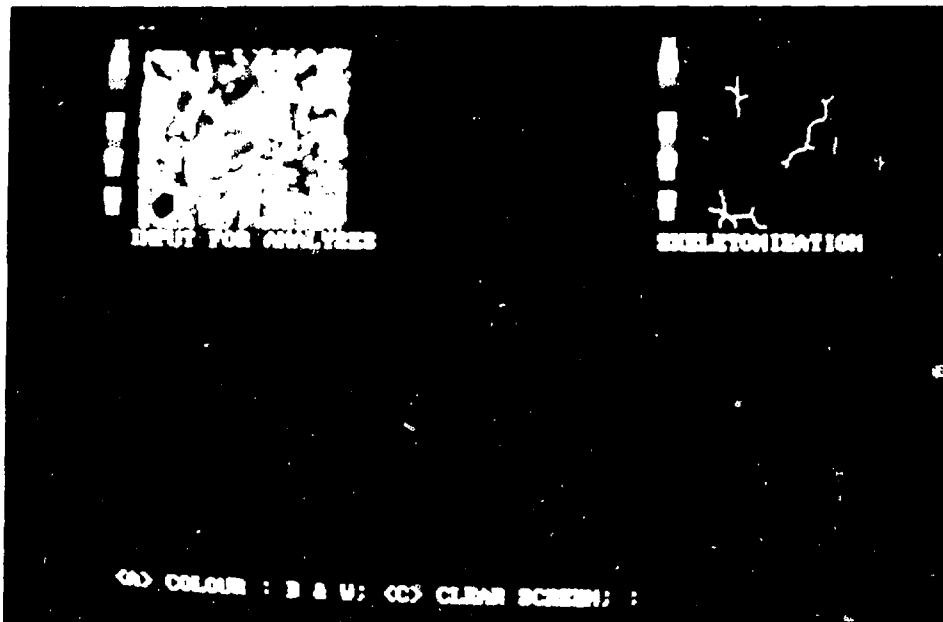cursor (Black and white image).
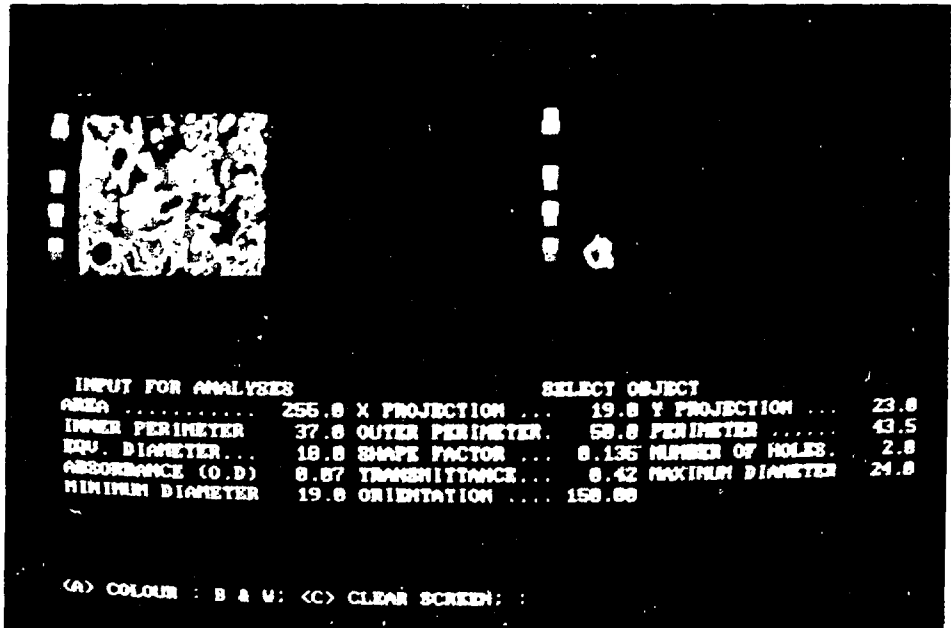
Fig 5 9 a Image data acquired with frame grabber from a SEM photograph of a metallurgical sample
(128 × 128)
5 9 b Binary image object pointed by graphic cursor (Fig 5 7 b) is isolated for feature measurement
shown in lower part

characterization of these objects is done through measurements of different features such as area, projections, shape factors etc. These measurements are then subjected to statistical analysis to arrive at reliable parameters.

VI CONCLUSIONS

To conceive image transformations from statistical approaches require greater understanding of not only statistical methods of image description but also the links between communication theories and signal processing. Based on such approaches, the information in the image, per se is maximized by adopting equiprobable distribution of grey levels in the picture: thus providing a scientific basis to imaging science & processing methods. Although grey level resolution could be increased by increasing the number of bits of video - digitisation or intensity levels, noise level present in the system imposes its restrictions to quantifying the information. Thus SNR is limited by a noise in the systems: and averaging of N - digital frames could be adopted to increase the limit by a factor of $\sqrt{N}$. The spatial resolution in principle is limited by the resolution in the matrix frame chosen for digitizing the spatial distances (e.g. 512x512 corresponding to a space of dxd cm^2). But, as mentioned in the introduction, the point spread function (PSF) actually limits the system resolution. If the PSF is invariant to spatial & temporal transformation, as is normally the case in linear, time invariant systems, the inter - pixel influences which is known a priori, could be eliminated to improve the image resolutions. Autoregressive (AR) methods is a step in this direction and is superior to conventional deconvolution

procedures. Such super - resolution techniques are becoming widely used in Image Processing: and the second report in this series will dwell on such topics.

References

1. Andrews, H.C., Tescher, A.G. and Kruger, R.P. (1972).
   Image Processing by Digital Computers."
   IEEE Spectrum, Vol. 9,pp 20-32.

2. Andrews, H.C. and Hunt B. (1977) Digital Image Restoration,
   Prentice-Hall, Englewood Cliffs, New Jersey.

3. Bracewell, R.N. (1984) "Fast Hartley Transform",
   Proceedings of IEEE, Vol. 72, pp. 1010-1018.

4. Cooley, J. W. and Tukey, J.W. (1965). "An Algorithm for the
   Machine Calculation of Complex Fourier Series",
   Math. of Comput. vol. 19, pp. 297-301.

5. Gonzalez, R.C. and Wintz, P. (1977)
   Digital Image Processing.
   Addison - Wesley, New York.

6. Hall, E. L. (1979) Computer Image Processing and
   Recognition, Academic Press, New York.

7. Haridasan, G. (1988), "Image Processing Activities and
   Their Applications in Nuclear Industry, Nuclear Medicine
   and Advanced Research Fields." Proc. National Symposium-
   cum-workshop on Advances in Imaging & Image Processing,
   and XII All India Convention of Biomedical Engineering
   Society Of India, Dec. 20-23. Bombay, pp. W-3.1 to W-3.7.

71

8. Haridasan, G. (1988), "A Review of Modern Imaging Modalities for Medical Applications", *Ibid.*, pp. W-3.1 to W-3.7.

9. Joshi, V.M., Patankar, V.H., Pednekar, S., Fernandes, I.A. and Haridasan, G. (1988), "Video Frame Data Acquisition - Hardware Developments", *Ibid.*, pp. S-III 1.1 to 1.4.

10. Joshi, V.M. (1988), "Functional Aspects & Features of Image Processing Systems", *Ibid.*, pp. S-VI 8.1 to 8.9.

11. Klingler, Jr., J.W., Vaughan, C.L., Fraker, Jr., T.D. and Andrews, L.T. (1988) "Segmentation of Echocardiographic Images Using Mathematical Morphology", IEEE trans. Biomed. Engg. Vol. BME-35, pp. 925-934.

12. Pratt, W. K. (1978) Digital Image Processing, Wiley, New York.

13. Rangayyan, R.M. (1988) "Digital Image Processing", Proc. National Symposium-cum-workshop on Advances in Imaging & Image Processing, and XII All India Convention of Biomedical Engineering Society Of India, Dec. 20-23. Bombay, pp. W-4.1 to W-4.24.

14. Rosenfeld, A. and Kak, A. C. (1976) Digital Picture Processing, Academic Press, New York.

15. Singh, B., George, J. and Haridasan, G. (1988),
    "Development of Image - Processing Software For Medical
    and NDT Applications", Proc. National Symposium-cum
    -workshop on Advances in Imaging & Image Processing, and
    XII All India Convention of Biomedical Engineering Society
    Of India, Dec. 20-23. Bombay, pp. S-III 4.1 to 4.8.

16. Singh, B., George, J. and Haridasan, G. (1988),
    "Development of Software For Binary Image Analyses",
    Ibid., pp. S-III 5.1 to 5.6.

17. Singh, B. (1985) Computer program for Graphical Display
    of Data. Technical Report B.A.R.C. /I-825.

18. Singh, B. (1985) A Computer Code for Three Dimensional
    Plot of A Sample From Bivariate Distribution. Technical
    Report B.A.R.C. /I-782.

19. Singh, B. (1979) Computer Code for Statistical Tests of
    Significance. Technical Report B.A.R.C. /I-531.

Fourier Transform: The Fourier transform of a 2 dimensional image is a suboptimal, orthogonal transform having a complex kernel defined as $\exp[-2\Pi j(ux+vy)]$, and the transform is given as

$$F(u,v) = \int \int f(x,y) \exp[-2\Pi j(ux + vy)] \, dx \, dy$$

where $F(u,v)$ is the Fourier transform of the image $f(x,y)$,

u,v the spatial frequency in x and y direction

respectively.

The inverse transform of $F(u,v)$ to obtain image $f^{\sim}(x,y)$ is given as

$$f^{\sim}(x,y) = \int \int F(u,v) \exp[2\Pi j(ux + vy)] \, du \, dv$$

The above equations are for continuous variables x and y. For the discrete case these equations can be written as follows for Fourier Transform,

$$F(k,l) = 1/N \sum_{m=0}^{N-1} \sum_{n=0}^{N-1} f(m,n) \exp[-2\Pi j(km + ln)/N]$$

and for inverse Fourier transform as

$$f(m,n) = 1/N \sum_{k=0}^{N-1} \sum_{l=0}^{N-1} F(k,l) \exp[2\Pi j(km + ln)/N]$$

The straight forward implementation require NxN complex multiplications and similar number of additions. If the number N can be made to be 2^n (by padding the vector by zeros), the symmetry in complex frequency plane can be used to a fast implementation of the transform. The Fast Fourier Transform (FFT) algorithm reduces these multiplications to $N \times \text{Log}_2 N$ which yields a significant reduction in the computational timings. The Fourier transform has some important and useful properties that are quite useful for simplifying mathematical formulations for many signal processing applications.

a) Linearity: Fourier transform of a linear sum of functions is a linear sum of the Fourier transform of individual functions. The input function $f(x,y)$ has the Fourier transform $F(u,v)$ given as

$$f(x,y) = \sum_{l=1}^{n} a_i \, f_i(x,y)$$

$$F(x,y) = \sum_{l=1}^{n} a_i \, F_i(u,v)$$

where $F_i(u,v)$ is the Fourier transform of function $f_i(x,y)$

75

b) Scale change: Scale change in variable x,y leads to inverse change in the corresponding frequency variable in the Fourier domain. The frequency and amplitude both are affected.

f(ax,by) leads to transform $1/|ab|$ F(u/a,v/b)

c) Shift of position: Shifting a spatial function in distance x=a leads to addition of phase by ua to the original phase. The magnitude is invariant to translation.

Mathematically f(x-a,y-b) in the spatial domain is equivalent to a linear shift of phase in the frequency domain given as F(u,v)exp(-j(ua+vb)).

d) Modulation: A spectrum will be centered around the frequencies of the sinusoid if the spatial function is multiplied by that particular sinusoid.

If the spectrum is to be centered about u_0 and v_0 , the frequency shift equation is F(u-u_0) and in space the same can be represented as f(x,y)exp(j(u_0x + v_0y).

e) Convolution: Convolution of any two spatial functions requires different steps like reversal, translation, multiplication and summation. But this operation in the frequency domain involves only direct multiplication of the two spectral functions.

In the spectral domain we write the operation as

```
N-1 M-1
 Σ   Σ  f(i,j)h(m-i,n-j)
i=0 j=0
```

where f and h are the two spatial functions used for convolution and the same in frequency domain is given as $F(k,l)H(k,l)$.

f) Correlation of two spatial functions is the same as the product of one of the spectrum and the complex conjugate of the other in the frequency domain.

The spatial correlation can be written as

```
N-1 M-1
 Σ   Σ  f(i,j)h(k-i,l-j)
i=0 j=0
```

and the corresponding equation in the frequency domain is

$F(k,l)H^*(k,l)$.

g) Multiplication: This is the inverse of case e where the product of the spatial functions produces the same results as the convolution of the functions in the frequency domain.

h) Rotation: Rotation of the input spatial image by an angle produces the original spectrum rotated by the same angle. If $f(m',n')$ is the rotated spatial image and $F(k',l')$ the rotated spectral image then we can write

$$m' = m\cos\Theta + n\sin\Theta$$

$n' = -m\sin\Theta + n\cos\Theta$

and $k' = k\cos\Theta + l\sin\Theta$

$l' = -l\sin\Theta + k\cos\Theta$

Θ is the angle of rotation.

i) Differentiation: This operation results in a high pass filter output. Differentiation operation in the frequency domain can be written as $(ju)^n F(u,v)$. For discrete cases in the space domain we have $f(m,n) - f(m-1,n)$ and the same in frequency domain is equivalent to the operation like $F(k,l)\{1-\exp(-jk/N)\}$ which is the differential operation for discrete cases.

j) Integration: This operation involves a similar type of process but it is a low pass filter and here the multiplier for the spectral component is $1/(ju)^n$, for an nth order integration operation. For discrete cases it is $f(m,n) + f(m-1,n)$ in space and $F(k,l)\{1+\exp(-jk/n)\}$ in the frequency domain.

.

APPENDIX 2

Karhunen Loeve Transform: This transformation is based on the statistical properties of the picture. It gives the minimum reconstruction error and so is called an optimum transform. The image is considered to be a random vector and it is characterized by 2 parameters, namely - "mean vector" and "covariance matrix".

If the covariance matrix of the input is CR_{xx} and if CR_{yy} is the covariance matrix of the transformed data, they can be expressed as

$$CR_{xx}= E[(X - M)(X - M)']$$

We represent the random image vector X by a transformation

$$X= \sum_{i=1}^{n} y_i A_i$$

Assuming A to be a non singular matrix with linearly independent basis vectors of n dimension, we can write Y as

$$Y= A'X = \sum_{i=1}^{n} A'_i x_i$$

If only m (m $\leq$ n) of the n components of Y which contribute to X are known then X can be approximately written as

$$X(m) = \sum_{i=1}^{m} y_i A_i + \sum_{i=m+1}^{n} b_i A_i$$

Thus the error introduced is

$$e = X - \hat{X} = \sum_{i=m+1}^{n} (y_i - b_i)A_i$$

The mean square error is thus

$$\overline{e^2}(m) = \sum_{i=m+1}^{n} E\{(y_i - b_i)^2\}$$

Solving the above for minimum mean square error we have

$$b_i = E\{y_i\} = A'_i E\{X\}$$

$$\overline{e^2}(m) = \sum_{i=m+1}^{n} E[(y_i - E\{y_i\})]$$

$$= \sum_{i=m+1}^{n} E\{A_i^{-1}(X - M)(X - M)'A_i\}$$

$$= \sum_{i=m+1}^{n} A_i^{-1} CR_{xx} A_i$$

If the basis vectors A_i are eigen vectors of CR_{xx} and if $A'_i A_i = 1$ we have

$$\alpha_i = A'_i CR_{xx} A_i$$

and the mean square error is

$$\overline{e^2}(m) = \sum_{i=m+1}^{n} \alpha_i$$

where A_i is the eigen vector and α_i the corresponding eigen value of CR_{xx}.

Thus the mean square error can be minimized by ordering the eigen values $\alpha_1 > \alpha_2 > \alpha_3 > \ldots\ldots\alpha_n$. i.e. if the component y_i is eliminated the mean square error increases by α_i. Therefore those components of y_i that correspond to the minimum eigen value can be neglected without causing much of the coding error. The procedure can be summarized by the following steps, 1) For a given vector X, find the covariance matrix CR_{xx}. 2) Find the eigen values α_i and the corresponding eigen vectors A_i , i=1,2,3,....,n. 3) Arrange these in ascending order of α_i. The covariance matrix for the transformed variable Y is given as CR_{yy} = A' CR_{xx} A is a diagonal matrix, implying that the vector Y has uncorrelated components. 4) The transformed vector Y can also be obtained from a subset of eigen vectors by ignoring the eigen vectors corresponding to small eigen values.

Walsh-Hadamard transform: This is also a suboptimal orthogonal transform with square wave transformation functions. These functions are real and they are described by their sequencies which is half the number of zero crossings in the interval (0,1). The coefficients of the representation are called sequency components. This transform is computationally fast because they involve only 1's and -1's. The Walsh functions are given by the relation

$$W_0(x) = 1 \quad ,$$

$$W_1(x) = \begin{cases} 1 & x < 1/2 \\ -1 & x > 1/2 \end{cases}$$

$$W_n(x) = \begin{cases} W_{n/2}(2x) & x < 1/2 \\ W_{n/2}(2x-1) & x \geq 1/2, \ n \text{ odd} \\ -W_{n/2}(2x-1) & x \geq 1/2, \ n \text{ even} \end{cases}$$

Here n/2 takes only the quotient part of the division and W_0, W_2, W_4,....etc. are even functions which are symmetric around x=1/2, and W_1, W_3,...etc. are the odd functions that are antisymmetric around x =1/2.

The Walsh functions should be sampled to have samples which are a power of 2 so that even and odd function pairing is possible. These matrices have the row ordered with the increasing number of sequency or the zero crossings. The Hadamard matrices

are also similar to the Walsh, but here the row ordering is different. The Hadamard matrices are easy to work with as the higher order matrices can be generated from a small core matrix of the form

$$H_2 = \begin{bmatrix} 1 & 1 \\ 1 & -1 \end{bmatrix}$$

The Hadamard matrix of order 2N can be generated recursively as

$$H_{2N} = \begin{bmatrix} H_N & H_N \\ H_N & H_N \end{bmatrix}$$

The 2 dimensional Walsh Hadamard transform of an input image f is given as $F = H[f]H$ where $H = 1/\sqrt{N}\ H_N$.

This transform is quite useful not only for image coding but also for pattern recognition, sequency filtering etc. As this transform considers all the image elements for computation of the transform coefficients, it is globally sensitive.

APPENDIX 4

Discrete Cosine Transform:This is also an orthogonal transform that comes under the sub optimal class with real valued transformation kernel. The basis vectors are sampled cosine functions and the transformation matrix is given as

$$H = 1/\sqrt{N} \ [H_{kl}]$$

where $H_{kl} =$
$$\begin{cases} 1, & l = 0 \\ \\ \sqrt{2}\cos\{(2k+1)l\pi/2N\} & k = 0,1,2....N-1 \\ & l = 1,2,.....N-1 \end{cases}$$

The basis vectors of DCT are related to the class of Chebyshev polynomials which are also orthogonal. The eigen vectors of a Toeplitz matrix and the DCT matrix are related by their basis vectors. This has a fast computation algorithm and it can also be computed from a 2N point FFT.

This transform is more efficient than the WH type as here the mean square error is minimal but it is quite slow computationally. The forward and the inverse transformation kernels are the same.

APPENDIX 5

Haar Transform: This is also an orthogonal sub optimal
transform which has elements 1, -1, 0 and powers of $\sqrt{2}$. The
matrix rows consider different elements of the vector, depending
on the row number in the computation of the transform
coefficients. The first coefficient is the mean of the vector,
the second is the difference of means for first half and the
second half elements of the vector. The remaining coefficients in
groups of power of two (2^k, k=1,2,3,4...,n-1) are weighted
(weight equal to $[\sqrt{2}]^k$) difference of means of the vector
elements at different positions of the vector and the element
count for averaging is given as 2^l l=n-2,n-3,...,1,0. For example
when the vector is of 4 elements, the third coefficient is
difference of first two elements weighted by $\sqrt{2}$ and the fourth
element is similarly weighted difference of third and fourth
element. It can be verified easily that for transform of N
element vector involves N(n+1) additions and $2+2^1+2^2+..$ $...+2^{n-1}$
multiplications.

The Haar transform is both globally and locally sensitive as
it involve the parts of the vector for computation of third and
subsequent coefficients of the transform.

For a NxN two dimensional matrix [f], the Haar transform [F]
is given as

[F] = 1/(NxN) [H] [f] [H]'

[f] = [H]'[f] [H]

where [H]' is the transpose of [H]

Slant transform: The Slant transform is another fast, suboptimal, orthogonal transform, which uses sawtooth waves in place of sinusoids or step functions for fitting the input data, leading to the transformed output image. The basis matrix S can be easily computed by the recursive relationship, involving the lower order slant matrix. The lowest order Slant matrix S(2) is defined as

$$S(2) = 1/\sqrt{2} \begin{bmatrix} 1 & 1 \\ 1 & -1 \end{bmatrix}$$

The recursive relationship for S(N) in term of lower order matrix S(N/2) is given as the product of matrices as shown below. Higher order matrix is obtained by appending zero partitions on the off diagonal parts, the main diagonal partitions are the lower order slant matrix. The matrix is premultiplied by another matrix obtained by adding identity matrices and zero matrices.

$$
\begin{bmatrix}
1 & 0 & . & Z(2xk) & . & 1 & 0 & . & Z(2xk) \\
a(N) & b(N) & . & & . & -a(N) & b(N) & . & \\
\hline
& Z(kx2) & . & I(kxk) & . & Z(kx2) & & . & I(kxk) \\
\hline
0 & 1 & . & Z(2xk) & . & 0 & -1 & . & Z(2xk) \\
-b(N) & a(N) & . & & . & b(N) & a(N) & . & \\
\hline
& Z(kx2) & . & I(kxk) & . & Z(kx2) & & . & -I(kxk)
\end{bmatrix}
\begin{bmatrix}
S(M) & . & O(M) \\
\hline
O(M) & . & S(M)
\end{bmatrix}
$$

where O(M) is zero matrix of M rows and M columns,

S(M) is lower M order slant matrix,

M = N/2

Z(ixj) is zero matrix with i rows and j columns,

k = M - 2,

a(N)= $\sqrt{[\ 3MxM/(4xMxM - 1)]}$

b(N)= $\sqrt{[(MxM-1)/(4xMxM - 1)]}$

For a NxN two dimensional matrix [f], the Haar transform [F] is given as

[F] = 1/(NxN) [S] [f] [S]'

[f] = [S]'[f] [S]

where [S]' is the transpose of [S] and [S] is slant matrix S(N) defined above.

Hartley Transform: It is an orthogonal sub optimal transform which has a real valued kernel. For input sequence $f(t)$, $t=0,1,2,....,M-1$, the Hartley transform $H(s)$ is given as

$$H(s) = \Sigma \ f(t)\,cas(2\Pi st/M) \qquad\qquad s=0,1,2,....,M-1$$

where $cas(\Theta) = cos(\Theta) + sin(\Theta)$

   s/M is similar to cycles per unit t

The FFT has the following decimation relationships

$$F^{\sim}(s) = \sum_{t=0}^{2M-1} f(t)\ exp(i\Pi st/M)$$

$$F^{\sim}(s) \qquad = F_e(s) + F_o(s)\ \ exp(-i\Pi s/M)$$

$$F^{\sim}(s \pm M) = F_e(s) - F_o(s)\ \ exp(-i\Pi s/M)$$

These relationships are used to compute the Fourier transform of 2N point sequence, $F_o(s)$ and F_e are Fourier transforms of odd and even indexed data points. The relationship between Fourier transform $F(s)$ and Hartley transform $H(s)$ is given as

$$F(s) = [\ H(s) + i\ H(-s)]/(1+i)$$

Using these relations even and odd indexed data can be

separated for Hartley transform, yielding

$$H^{\sim}(s)+iH^{\sim}(-s) = [H_e(s)+iH_e(-s)]+[H_o(s)+iH_o(-s)].$$
$$\exp(-i\Pi s/M)$$

This equations can be separated in to real and imaginary parts as

$$H^{\sim}(s) = H_e(s)+H_o(\ s)\cos(\Pi s/M)+H_o(-s)\sin(\Pi s/M)$$

$$H^{\sim}(-s)= H_e(-s)+H_o(-s)\cos(\Pi s/M)+H_o(\ s)\sin(\Pi s/M)$$

The power spectral density function can be directly obtained from Hartley transform without conversion to FFT as

$$P(s) = [H^{\sim}(s)^2 + H^{\sim}(-s)^2]\ /2$$

The $^{\sim}$ operator denote the transform on 2M points. Thus Hartley transform is quite similar to the DFT , but has no complex term involved in it and therefore it is quite fast and efficient. It can be computed using the FFT also. The advantages of Hartley transform over FFT for real data are 1) require only half the array space, 2) has identical forward and inverse transforms, 3) more direct conversion to power spectral density function.

APPENDIX 8

SOFTWARE DEVELOPMENTS FOR BINARY IMAGE ANALYSES

Following programs have been developed for binary image
analyses.

GRAY LEVEL IMAGE OPERATIONS

Read input image from file:- The grey level image is read from
the user specified file.

Acquire new grey image:- The analyses performed on earlier
image is saved in appropriate memory area and the new grey level
image is read from the user specified file.

GENERATE BINARY IMAGE BASED ON SPECIFIED GREY LEVELS: The user
specified window on grey scale is used to get a binary image.

DISPLAY THE OUTPUT (GREY) LEVEL: The gray level image along
with the binary image in output array are displayed on the
terminal.

DISPLAY DISTRIBUTION: The distribution of the parameter
measured on individual objects along with the grey level image,
binary image in the output array and the statistics are displayed
on the terminal.

BINARY IMAGE AND BIT PLANE OPERATIONS: The binary image in the
output array and the binary image stored as bit plane in Imb

array are operated upon. The different operations are

Store output (binary image) in bit plane:- Output image to the user specified bit plane.

Move bit plane :- Source bit plane to the destination bit plane.

Clear a bit plane:- Destination bit plane is cleared.

Set mask bit plane:- Output array is set in the mask bit plane.

Clear mask bit plane:- Mask bit plane is cleared.

PREMEASUREMENT PROCESSING: To weed out the noise from binary image before making measurements.

LOGICAL OPERATIONS

Inclusive OR of bit planes:- Destination bit plane equal to the OR of source and destination bit planes.

Exclusive OR of bit planes:- Destination bit plane equal to the exclusive OR of source and destination bit planes.

AND of bit planes:- Destination bit plane equal to the AND of source and destination bit planes.

Negate a bit plane:- Destination bit plane equal to the NOT of source bit plane.

MORPHOLOGICAL PROCESSING: A structural element is used to

modify the destination bit plane and result is set in the output image array.

Dilate bit plane:- Destination bit plane is dilated increasing the size of the binary objects.

Erode bit plane:- Destination bit plane is eroded decreasing the size of the binary objects.

Thicken operations:- Destination bit plane is dilated increasing the size of the binary objects. The objects in the output image are not allowed to touch each other.

Reconstruct plane:- The binary objects in destination plane are modified till they attain the size of the corresponding objects in source bit plane.

Close holes:- The holes in the binary objects are filled with ones, making them (holes) indistinguishable from the object.

Remove objects on the border:- Objects on the border are removed, leaving the image with the objects well within the borders.

Overture (open up) a bit plane:- The destination bit plane is eroded by the specified count and then dilated by the same count.

Fermeture (close) a bit plane:- The destination bit plane is dilated by the user specified count and then eroded by the same count.

Skeletonisation:- The output image is processed so that objects are reduced to the minimum size, without breaking the objects.

Axes of local symmetry:- The objects are reduced to the line segments that are axes of symmetry for each object.

Binary image refinement:- Using maxmin filter the objects falling within the filter window are removed leaving the other objects unaltered.

AREA SEGMENTATION: Different parts of binary image are isolated for measurements on the objects included in the selected part.

Select object:- Object specified by the user through graphic cursor or by the coordinate is isolated.

Delete object:- Object specified by the user through graphic cursor or by the coordinate is removed from the binary image.

Connect points in a bit plane:- Joins the points by a line passing though the user specified points. The bit along the line is either cleared, set to 1 or reversed.

Select/remove part by contours:- Area of the image masked by the linear segments making closed contours, is either selected or removed as specified by the user.

MEASUREMENTS ON INDIVIDUAL OBJECT: the following measurements are made on the individual object isolated from the rest of the image.

```
AREA
X PROJECTION
Y PROJECTION
INNER PERIMETER
OUTER PERIMETER
PERIMETER
EQUIVALENT DIAMETER
SHAPE FACTOR
NUMBER OF HOLES
ABSORBANCE (OD)
TRANSMITTANCE
MINIMUM  DIAMETER
MAXIMUM  DIAMETER
SLOPE
```

GLOBAL MEASUREMENTS:
The following measurements are on the whole of the binary image with all the objects.

```
GLOBAL AREA OF THE OBJECTS
GLOBAL EQUIVALENT DIAMETER
GLOBAL NUMBER OF HOLES
COUNT  THE  OBJECTS
```

ANALYSES: The measurements on the objects are used to generate the histogram, check the type of distribution and perform statistical analyses.

Histogram:- Histogram on any of the measurement can be generated.

Object erosion size histogram:- The distribution of the objects based on the number of erosion to remove the object, is

generated.

Statistical analyses of data:- The following analyses options are available.

i) Type of distribution (normal or log-normal).

ii) Correlation among any two parameters.

iii) Inter-image comparison of measurements with Analyses of Variance (ANOVA).

Arrange objects in order:- The grey level image of the binary objects is isolated and arranged in a sequence based on the measurement on the binary object.

Grey level profiles through a pixel:- Also the grey level profiles through a point can be obtained.